Title

Toward Carbon Negative, Sustainable Chemical Manufacturing by upgrading ethanol and other simple carbons using a cell-free platform.

Permalink

https://escholarship.org/uc/item/82h376sn

Author

Liu, Hongjiang

Publication Date

2022

Peer reviewed|Thesis/dissertation

UNIVERSITY OF CALIFORNIA

Los Angeles

Toward Carbon Negative, Sustainable Chemical Manufacturing by upgrading ethanol and other

simple carbons using a cell-free platform.

A dissertation submitted in partial satisfaction of the

requirements for the degree Doctor of Philosophy

in Biochemistry, Molecular and Structural Biology

by

Hongjiang Liu

2022

ABSTRACT OF THE DISSERTATION

Toward Carbon Negative, Sustainable Chemical Manufacturing by upgrading ethanol and other simple carbons using a cell-free platform.

by

Hongjiang Liu

Doctor of Philosophy in Biochemistry, Molecular and Structural Biology

University of California, Los Angeles, 2022

Professor James U. Bowie, Chair

To produce more diversified and more valuable commodities from a biobased economy, I have sought to upgrade ethanol into a wider range of products through cell-free platform technologies. I have built two styles of ethanol valorization system, one through acetaldehyde condensation, another through acetyl-CoA. Also, I have developed methods to power biochemical systems, one that converts electrical power into reducing equivalents and another that can regenerate ATP while co-producing acetone. I developed a 1,3-BDO production system that reached a maximum 0.16 g/L/h productivity, and, with replenishment of feedstock and enzymes, achieved a 1,3-BDO titer of 7.7 g/L. I also developed an isoprenol production system able to reach a maximum 1.0 ± 0.05 mM/h productivity and 12.5 ± 0.8 mM maximum titer. My ATP generator reached titers of 27 ± 6 mM ATP and 59 ± 15 mM acetone with maximum ATP synthesis rate of 2.8 ± 0.6

mM/hour and acetone of 7.8 ± 0.8 mM/hour. These results demonstrate a proof-of-concept

blueprint for more diversified bioeconomy for commodity chemical productions.

The dissertation of Hongjiang Liu is approved.

Chong Liu

Robert Thompson Clubb

Robert P. Gunsalus

James U. Bowie, Committee Chair

University of California, Los Angeles

2022

Dedication

It has been a little over five years of eventful journey. We have witnessed the COVID19 pandemic unfolding on a global scale, we have witnessed the wild ride of 2021 Jan 6th capitol hill attack, we have witnessed our world changing right under our feet. Let it be known that it is through perseverance we live and thrive. To this end, I want to thank everyone who has been on this journey with me. Especially my younger brother Hongtao "Derrick" Liu and my mother Qing Yan, and the rest of my family, your company is the fountain of my joy, my pride, and my inspiration. Also, Professor Bowie, you have been the best mentor I could have ever asked for, you have helped me to grow, not only as a scientist, but also a person. Your wisdom and your character will be a towering beacon ever in my career, and I look forward working with you more in the future. Lastly, I want to express my most sincere gratitude to all the amazing friends I have met in the UCHA Co-op home, you made every moment as enjoyable as it can be.

Acknowledgements

TABLE OF CONTENT

VITA

Experience

2016 September – 2022 March (expected)

Graduate Student Researcher, UNIVERSITY OF CALIFORNIA, LOS ANGELES

I have achieved producing useful and valuable chemicals by upcycling ethanol and developed a platform cell-free technology for carbon recycling based on complex enzymatic cascades. My research is funded by multiple DoE contracts. I have published 4 articles and led team of students and collaborators in a highly cross-disciplinary setting. I am familiar with wide range of molecular biology and biochemical methodologies.

2018 December – 2020 June

Teaching Assistant, UNIVERSITY OF CALIFORNIA, LOS ANGELES

I have led hands-on laboratory practice class for upper division students. I have earned consistently 90%+ good reviews from my students. I have excelled in communicating with a diverse group of students with cultural and linguistic sensitivity.

Education

Ph.D.(candidate), UNIVERSITY OF CALIFORNIA, LOS ANGELES   2016 – 2022

B.S., SICHUAN UNIVERSITY   2012 – 2016

Honor and Awards

Hult Prize Winner	2021
UCLA-CSST section leader	2018
Excellence in Chemistry Ph.D. award	2016
CSC-UCLA scholarship	2016
UCLA-CSST grant	2015
4x China National Pilot Program Award	2012 – 2016

Publications

1. Liu, H., Bowie, J.U. Cell-free synthetic biochemistry upgrading of ethanol to 1,3 butanediol. Sci Rep 11, 9449 (2021). https://doi.org/10.1038/s41598-021-88899-w

2. Liu, H., Arbing M., Bowie, J. U. Expanding the use of ethanol as a feedstock for cell-free synthetic biochemistry by implementing acetyl-CoA and ATP generating pathways. (submitted)

3. Sherkhanov, S., Korman, T. P., Chan, S., Faham, S., Liu, H., Sawaya, M. R., . . . Bowie, J. U. (2020). Isobutanol production freed from biological limits using synthetic biochemistry. Nature Communications, 11(1). doi:10.1038/s41467-020-18124-1

4. Bowie, J. U., Sherkhanov, S., Korman, T. P., Valliere, M. A., Opgenorth, P. H., & Liu, H. (2020). Synthetic Biochemistry: The Bio- inspired Cell-Free Approach to Commodity Chemical Production. Trends in Biotechnology, 38(7), 766-778. doi:10.1016/j.tibtech.2019.12.024

Introduction

Carbon emission reduction is of global urgency

According to the United Nations, the world population will reach 8.5 billion by the year 2030 and over 10 billion by 2100[1]. The growing population exerts an enormous amount of pressure on carbon footprint. However, with COP21(Conference of Parties 21st summit) and other international treaties on limiting carbon dioxide emission taking effect, there is a growing drive to find alternatives to the fossil-carbon that can provide the necessary materials for sustainable development. Indeed, the chemical industry is a major producer of global warming gases, with 99% of carbon compounds derived from petroleum[2]. Utilization of captured carbon feedstock for chemical production could potentially provide a 10% reduction in global carbon emissions (3.5 GT CO_2-eq)[3]. Replacement of the carbon in organic molecules with carbon captured from CO_2 could therefore be an important component of a truly sustainable future economy[2–4].

To this end, many projects have been initiated by governments and companies around the world to different level of success[5]. In the decades leading up to this thesis, three main ways of capturing and utilizing emission from the sources mainly in the form of CO_2, CO and CH_4 or directly from the atmosphere have been developed. These are plant photosynthesis[6,7], microbial fermentation[8], and electrochemistry[9] such as seen in figure 1.
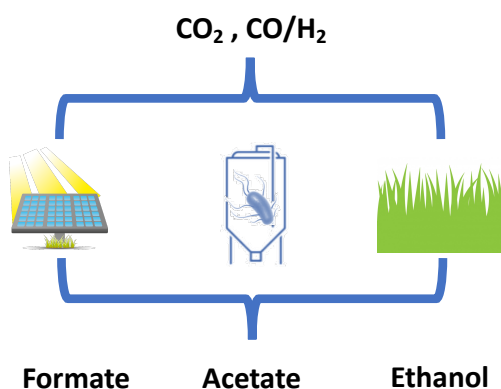
Figure 1) Carbon emissions are mainly captured in three ways through either electrochemistry or microbial fermentation, or agriculture and the main products are formate, acetate, and ethanol.

Some prominent examples exist such as traditional photosynthesis by corn and sugarcane harvesting for bioethanol production[10,11]. Or the capture of flue gas for fermentation by microorganisms to produce ethanol and acetic acid. Or leveraging new technologies, such as DAC (Direct Air Capture) technologies[12], to directly fix atmospheric CO_2 and then use electrochemical reduction to directly fix CO_2 into ethanol, formic acid, or small aldehydes[9]. Nevertheless, these processes can only produce simple carbon compounds such as ethanol/formate/acetate efficiently to date (reasons will be discussed later). These products are marginally useful. Ethanol is a relatively poor fuel, with low energy density and high-water content. Furthermore, ethanol can only be blended up to ~10% without engine modification[13]. Acetic and formic acids are only marginally industrially interesting. Combined, the lack of further upgrades of simple carbon compounds has limited the development and adoption of carbon-capture technologies.

The gap between bioethanol to high value products

While the upstream technologies that can fix carbon into simple carbon neutral or carbon negative chemicals have been in development for many decades and leaps of progress have been made, there exists a significant gap that we will need to address: we need to further valorize these rudimentary materials.

2
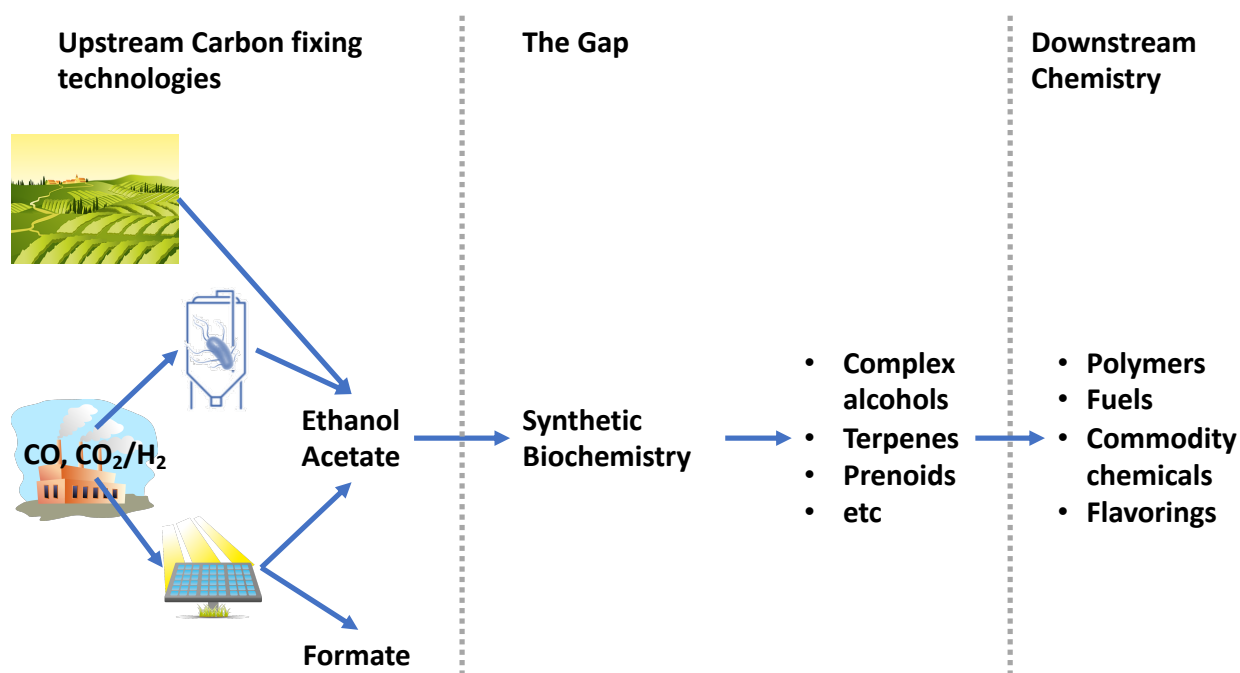
Figure 2) Synthetic Biochemistry is situated between upstream technologies that are rapidly maturing to produce low value yet bulk volume chemicals and downstream technologies that are already mature in processing commodity chemicals.

This gap between what we can do with current state-of-the-art fermentation or electrochemical processes with what the industry needs, is what I seek to bridge by upgrading small organic carbons to more sophisticated and valuable products (see figure 2, the gap).

Hence, I have sought to build more diverse chemicals from ethanol and acetate, with the help of an external power source if needed. From a direct observation of current development of cell-free technologies and surrounding industries, using ethanol, acetate and formic acid is advantageous in many ways. Here I will explore the high-level planning of these three molecules.

Using ethanol and acetate to build high value and more complex products is advantageous in two ways. One, it will help to address the utility problem of the first-generation biofuel technologies, namely ethanol is a relatively poor target product. By upgrading ethanol, more utility can be liberated, making the whole upstream industries around ethanol fermentation more viable. Two, we can make safe assumptions that ethanol would be abundantly available in the future and many mature technologies have already been developed around ethanol fermentation[14]. By joining forces with mature technologies, the technology to market cycle for my cell-free system potentially would be shorter and cheaper. Using acetate as building block follows along similar rationale. More importantly, in some processes that produces ethanol, acetate is a byproduct. Hence, upcycling acetate that is co-produced in ethanol fermentation is a natural path that is worth exploring. Obviously, this is a broad-stroke observation, and real commercial scale deployment is still yet to be seen[15–17]

In many instances, biochemical systems need to expend reductive energy to build complex molecules through catabolic reactions. To drive these reductive catabolic reactions, most commonly, NAD(P)H is expended in biology. Hence, the problem becomes how to generate these reducing cofactors while only using the small molecules the existing upstream technologies can readily produce? One promising way to generate the consistent NAD(P)H driving force is to use formic acid with formate dehydrogenase (FDH). FDH readily converts formic acid back to CO_2 while reduce $NAD(P)^+$ back to the reduced cofactors. Using formic acid as the reducing power offers other benefit in the cell-free context. One, formic acid can potentially be produced through electroreduction of CO_2.[18] So formic acid can act as a battery that stores electricity. If the

4

electricity is from solar or wind or other renewable sources, then the storage of such electricity in

formic acid would be beneficial in the long-term storage problem of renewable electricity[19].

Moreover, sometimes formic acid can be used as a building block to build more complex

materials though biochemical reactions[20]. Hence, I have set out to design and build a series of

biochemical systems surrounding the utilization of ethanol, acetate, and formic acid.

The unique advantage of synthetic biochemistry

Synthetic biochemistry or cell-free biochemical processes pose unique comparative advantages[21]

in fulfilling the role of upgrading simple organic carbon into useful industrial precursors and

commodities. Compared to pure electrochemical or fermentative processes, synthetic

biochemistry allows for high conversion efficiency, because unlike the complex metabolic

environment in cells, non-productive side reactions are essentially absent in a cell-free system.

While engineering cells to eliminate as many non-productive pathways as possible is a valid

approach, there is a physiological limit to the extent that engineering can keep the cells alive.

Cell-free systems from the ground-up don't need to consider life/death. In synthetic

biochemistry, design-build-test cycle can be much faster since it is easy to swap out individual

enzymatic components to test pathways. While traditional metabolic engineering per se is a

slower process. Genetic manipulation is slow and the intricate genetic circuitry interactions

makes modelling and predictions difficult. To build long pathways necessary to build complex

products, the difficulty in testing these pathways in cells compounds very quickly. Lastly,

without cells, there are no product or intermediate toxicity problems if the enzyme catalysts are

stabled in the given condition. While in living cells, product toxicity or deleterious effects of the

genetic manipulation all must be carefully considered, and often lead to low titer of final product or the impossibility of certain chemicals to be produced. For instance, many terpenes are toxic to cells, or deletions made in the central pathways are often detrimental to the host organism.

In parallel development to synthetic biochemistry, another idea is to use electrochemical catalysis to directly energize these small organic carbons. However, that it is very difficult to control the carbon-carbon bond formation which increasingly become harder with more complex carbon-chains in the more complex products. Generally, it is only efficient up to one or two carbon long.

Hence, in all, the advancements showed that synthetic biochemistry is a promising technology to bridge the gap between small low complexity, and low value ethanol/acetate to high complexity high value products. We are already seeing encouraging developments in the field of Synthetic Biochemistry or sometimes called Cell-Free biotechnologies. Teams around the world have made stride in designing new and more complex cell-free systems to produce value-added products. Such as development made by the Chinese Academy of Sciences, team of researchers were able to build starch from methanol using cell-free platform technologies[22] . Or such as Debut™ Biotech[16] where they as recent as August 12th 2021 raised a $22.6 million series A funding[23] to commercialize cell-free technologies. Or Percival Zhang's team able to scale to 20,000L reactor scale for cell-free myo-inositol production[24]. And such as, recent advancement made in J. Bowie's team[25], where cell-free production of isobutanol was able to reach more than 20x the cellular toxicity limit.

However, the synthetic biochemical systems are limited by three fundamental key factors. One, the enzyme catalysts must be stabilized to handle prolonged reactions and potentially harsh conditions. Two, cofactor use needs to be conservative to be commercially sensible. Three, the thermodynamic driving forces must be generated *in situ*. Indeed, throughout this thesis, a running theme is to tackle these three challenges.

Two systems of ethanol upgrade

Here I have attached two pieces of my primary research to further illustrate the ethanol

upgrading concept. For the readers convenience, I have reformatted the articles so that all the

figures were renumbered, and all the methodology and bibliography sections are combined. The

first chapter will discuss the construction of ethanol upgrade with aldehyde condensation as the

core mechanism. The second chapter will discuss using acetyl-CoA as the intermediate to

produce ATP and other products through ethanol.

Chapter 1, Synthetic biochemistry upgrading of ethanol to 1,3 butanediol

Hongjiang Liu and James U. Bowie*

Department of Chemistry and Biochemistry, Molecular Biology Institute, UCLA-DOE Institute,

University of California, Los Angeles, CA

*To whom correspondence should be addressed

Boyer Hall

University of California, Los Angeles

611 Charles E. Young Dr. E

Los Angeles, CA 90095-1570

bowie@mbi.ucla.edu

Competing Interests: JUB has co-founded a company, Invizyne Technologies, that seeks to develop cell-free chemical production methods. HL declares no competing interests.

Author Contributions: HL and JUB conceived of the project, analyzed results and wrote the manuscript. HL conducted all the experiments.

Abstract

It is now possible to efficiently fix flue gas CO/CO_2 into ethanol using acetogens, thereby making carbon negative ethanol. While the ethanol could be burned as a fuel, returning the CO_2 to the atmosphere, it might also be possible to use the fixed carbon in more diverse chemicals, thereby keeping it fixed. Here we describe a simple synthetic biochemistry approach for converting carbon negative ethanol into the synthetic building block chemical 1,3 butanediol (1,3-BDO). Our pathway is completely carbon conserving and can ultimately be powered electrochemically via formate oxidation. Our proof-of-principle system reached a titer of 7.7 g/L with maximum productivity of 0.16 g/L/h and maximum conversion efficiency of 85%. We identify a number of elements that can be addressed in future work to improve both cell-free and cell-based production of 1,3-BDO.

Background

The chemical industry is a major producer of global warming gases, with 99% of carbon compounds derived from petroleum[2]. Utilization of captured carbon feedstock could potentially provide a 10% reduction in global carbon emissions (3.5 GT CO_2-eq)[3]. Replacement of the carbon in organic molecules with carbon captured from CO_2 could therefore be an important component of a truly sustainable future economy[3,4,2].

Ethanol is one of the most important bio-based chemicals and is the prototype first-generation biofuel. Corn-based ethanol produced by standard yeast fermentation is currently the major source of bio-ethanol, and provides an estimated 20% reduction in greenhouse gas emissions

10

relative to gasoline[26]. New advances enable more dramatic reductions in emissions. In particular, commercial plants are being developed that employ acetogens to fix carbon from the atmosphere by converting flue gas or biomass syngas into ethanol[27,28], potentially providing a remarkable 98% reduction in greenhouse gas emissions relative to petroleum fuel[29]. Additionally, advances in electrochemical carbon capture allow efficient conversion of CO_2 into formaldehyde and formate[9,30]. A recent report also describes a method for efficient electrochemical conversion of CO_2 to ethanol[31]. To the extent that the electricity used in electrochemical conversions is derived from solar or nuclear plants, electrochemistry provides another carbon negative process for making simple carbon compounds. Yet ethanol and formate currently have very limited uses due to their lack of chemical complexity and reactivity. As a result, developing effective ways to upgrade simple molecules like formate and ethanol into more diversified chemicals could potentially form the basis for a more carbon efficient chemical industry by displacing chemicals derived from petroleum[27].

One approach to increasing product complexity of the carbon negative acetogenic process is by metabolically engineering acetogens to generate more complex chemicals[27]. Yet while a metabolic engineering approach is straightforward in theory, in practice there are many hurdles that must be overcome for commercial viability [32–34]. Cost-competitive production of next generation biofuels or bulk chemicals by fermentation using engineered microbes has proven to be extremely difficult. A major challenge is the loss of carbon during feedstock conversion, thereby wasting costly input biomass. For example, in the conversion of glucose to ethanol using standard glycolysis only four of the six carbon atoms end up in the ethanol product

and two are lost as CO_2. While it may be possible to introduce more carbon-conserving

pathways such as the non-oxidative-glycolysis pathway, reconfiguring central metabolism is far

from trivial[35,36].

Another possible approach to upgrading ethanol into more diverse products is to free ourselves

from cells and employ enzyme pathways, an approach we call synthetic biochemistry[21,25]. In a

pioneering effort, Zhang et al. developed a system to enzymatically convert ethanol into 2,3-

butanediol and 2-butanol[37]. They first employed alcohol dehydrogenase to make acetaldehyde,

which was then combined using a non-natural enzyme to make the 4-carbon molecule acetoin.

Acetoin could then be reduced with dehydrogenase enzymes to make 2,3-butanediol or 2-

butanol. In their system the reduction steps were powered by the oxidation of ethanol,

generating NAD(P)H. Because 2,3-butanediol and 2-butanol require different reducing

stoichiometry, Zhang et al employed the purge valve concept[38] to regulate the levels of NADPH

generated in the alcohol dehydrogenase step. A limitation of powering the required reduction

steps with ethanol oxidation is that the overall reaction is at the mercy of the overall

thermodynamics. For example, the 2,3-butanediol conversion (2 ethanol + NAD^+ = 2,3-

butanediol + NADH) is an unfavorable reaction under standard state conditions ($\Delta G'^m$ = 33

kJ/mol, where $\Delta G'^m$ is the free energy change at 1 mM standard state and pH 7.0)[39].

Nevertheless, the purge valve system did prove effective in these examples.

Here we introduce a different approach to more flexibly deploy reducing equivalents, a way to

power the reduction steps electrochemically, and we expand the range of molecules that can be

12

made from ethanol to 1,3-BDO. In our approach, the ethanol oxidation and subsequent reduction steps are separated and we provide reducing equivalents by the oxidation of formate. As formate can be produced electrochemically from CO_2, it introduces a way to indirectly power biochemical pathways by electricity. To make 1,3-BDO from ethanol we deploy a non-natural pathway conceived and developed by Yakunin and coworkers[40–42].
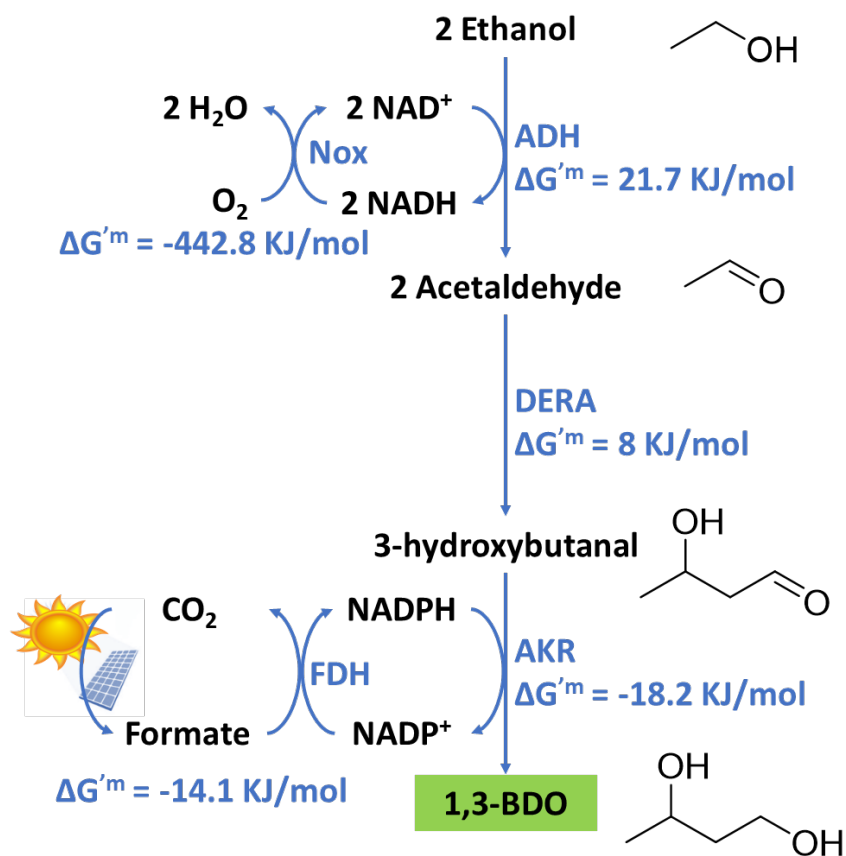
System Design

Figure 3. System design) Chemicals are shown in black text and enzymes in blue text. The standard state free energies for a 1 mM standard state and pH 7 are calculated using eQuilibrator[39].

Our system for 1,3 butanediol production from ethanol is shown in Figure 3. Ethanol is first oxidized to acetaldehyde via alcohol dehydrogenase (ADH). Ethanol oxidation is highly unfavorable thermodynamically with a $\Delta G'^{m} = 21.7$ kJ/mol [39]. Thus, we need a mechanism to drive the reaction forward. To accomplish this goal, we introduce an enzyme NADH Oxidase (Nox) that re-oxidizes NADH back to NAD^{+}. In this manner, a large NAD^{+}/NADH gradient is maintained that can drive the conversion of ethanol to acetaldehyde. To convert acetaldehyde into 1,3-BDO we used the pathway developed by Yakunin and coworkers[40–42]. To join acetaldehyde to make 3-hydroxybutanal (3-HBal) we employ a promiscuous aldolase 2-deoxy-D-ribose-5-phosphate aldolase (DERA) [43]. DERA naturally catalyzes the reversible breakdown of 2-deoxy-D-ribose-5-phosphate to glyceraldehyde 3-phosphate and acetaldehyde. DERA, however, can also catalyze an analog of the reverse reaction, to combine multiple units of acetaldehyde to hydroxyl-aldehydes such as 3-HBal [40,41,44]. Finally, 3-HBal is reduced to 1,3-BDO using a specific aldo-ketol reductase (AKR) identified by Kim et al.[42]

To supply reducing equivalents in the form of NADPH to the biosynthetic (reductive) phase of the pathway, we employ formate dehydrogenase (FDH). In this reaction formate is converted to CO_2. As CO_2 can be efficiently converted back to formate electrochemically[9], this step could ultimately be carbon neutral by using solar or nuclear power. Overall, by using carbon fixed into ethanol using acetogens and by powering the biosynthetic reactions using carbon neutral energy stored in formate, the system can provide carbon negative 1,3-BDO, and ultimately other carbon negative chemicals. The specific enzymes employed in this work are described in Supplementary Information.

14

We first tested the effectiveness of Nox for driving the generation of acetaldehyde. As shown in Figure 4, the addition of Nox allows for increased production of acetaldehyde. Starting with 100 mM ethanol and 2 mM NAD^+, in the absence of Nox, the acetaldehyde concentration reached a plateau of ~1.5 mM within 10 min and didn't increase substantially over the course of an hour. However, in the presence of Nox, the acetaldehyde concentration reached higher levels throughout the time course, increasing to 2.8 mM by 1 hour. Thus, Nox is effective in boosting acetaldehyde production as expected. We note that in the presence of Nox, the concentration of acetaldehyde jumps initially and then begins to increase steadily. This result may be due to rapid depletion of oxygen in solution followed by a rate limited by oxygen diffusion into reaction, although we did not investigate further.
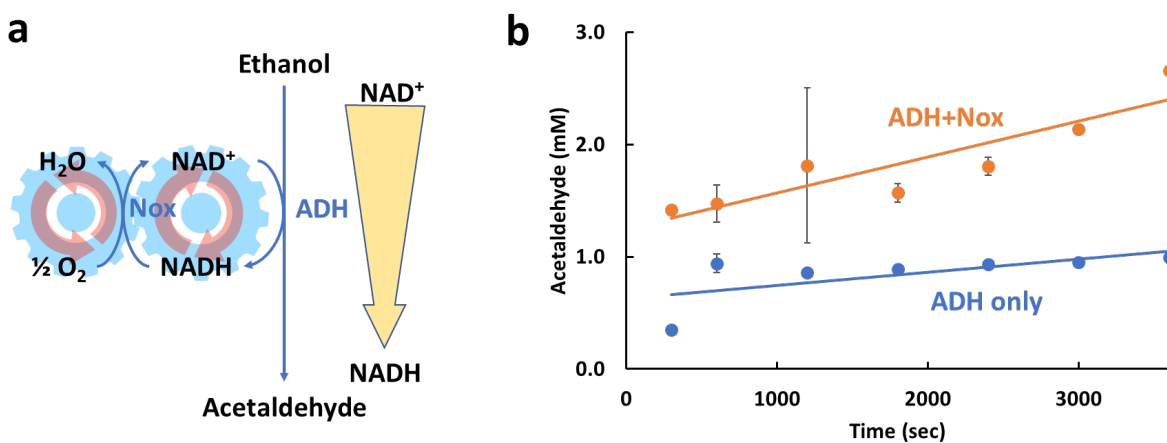
Figure 4. Ethanol Oxidation Module. a) The reaction scheme employed emphasizing the reaction is driven by the NAD^+/NADH gradient generated by the Nox re-oxidation of NADH to NAD^+. **b)** Acetaldehyde production with and without Nox. Production is improved by the introduction of Nox. Error bars reflect standard deviations of biological triplicates.

We next tested the biosynthetic phase of the system in which we convert acetaldehyde to 1,3 butanediol by supplying acetaldehyde and NADPH directly. As shown in Fig. 5, when we add

acetaldehyde to a mixture of DERA and AKR, we see a rapid conversion of NADPH to NADP$^+$

indicating the production of 1,3-BDO. However, we also found that when DERA is left out of

the reaction there is still some oxidation of NADPH by AKR alone suggesting that AKR is

somewhat promiscuous and can reduce acetaldehyde back to ethanol, albeit at a lower rate. The

substrate specificity of AKR is discussed further below.
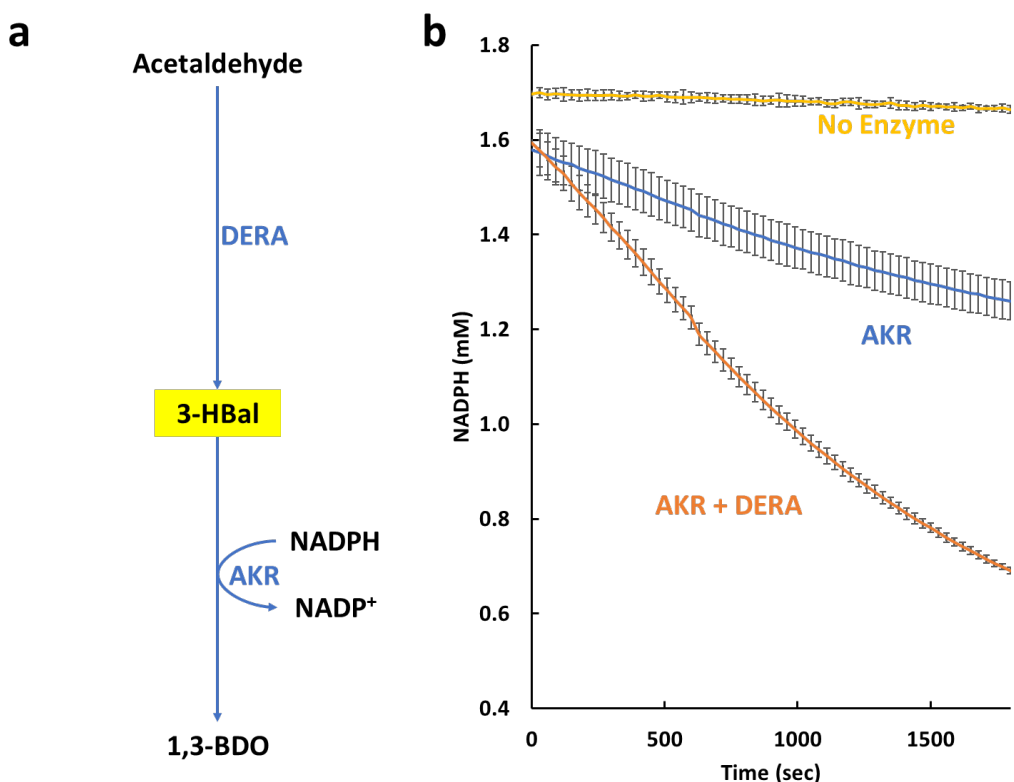
Figure 5. Reduction module, a) Schematic of the reductive module leading to 1,3-BDO. **b)**
Oxidation rates of NADPH in the presence of AKR only or AKR and DERA. The rate of
oxidation is greatly enhanced in the presence of DERA, indicating the production of 3-HBal.

Implementation of the full pathway:

With both the oxidative and the reductive modules tested, we next built the full system (Fig. 3)

by putting the oxidative and reductive modules together and adding NADPH generation via

formate dehydrogenase. The initial conditions based on intuitive guesses for enzyme

concentrations successfully produced 1,3-BDO, albeit only 1.6 mM after 1 day. To optimize the

system, we varied enzyme levels. In each optimization round we doubled and halved every

enzyme independently. The highest titer enzyme loadings were then used to initiate the next

round of optimization. After 7 rounds of optimization we saw a 25-fold titer improvement to ~40

mM after 1 day.
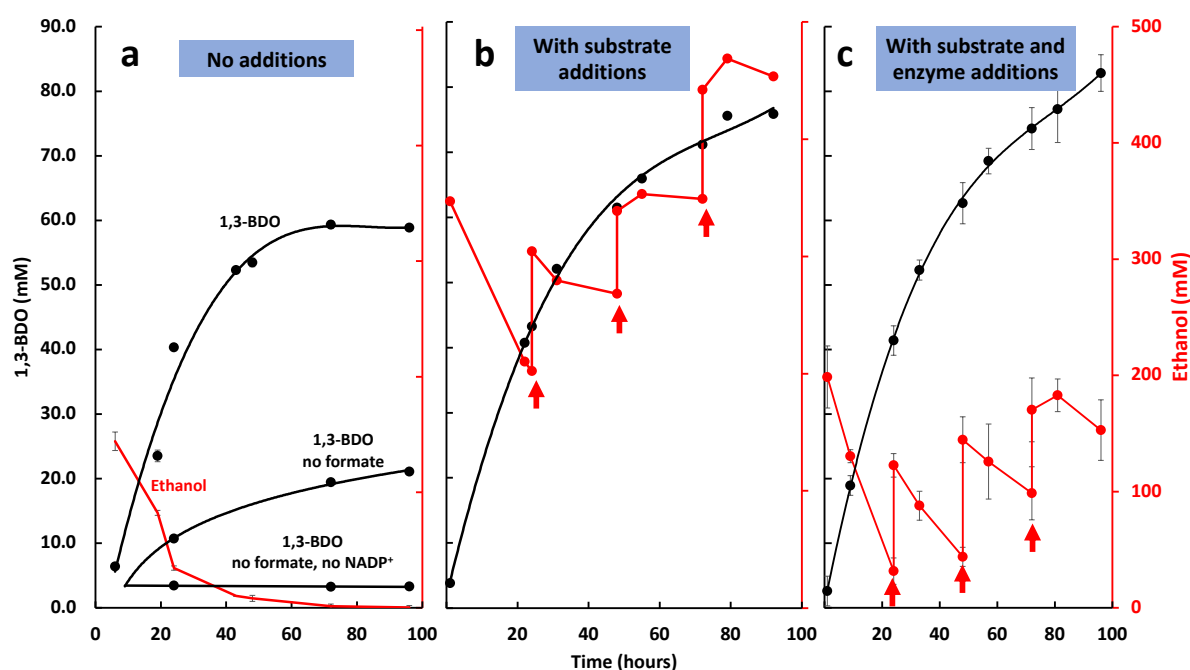
Figure 6. Conversion of ethanol to 1,3-BDO) Results for implementation of the full system described in Fig. 1 are shown. The 1,3-BDO concentrations are shown in black and ethanol concentrations are shown in red. **a)** Results for the full system including results leaving out formate or leaving out formate and $NADP^+$. **b)** The same implementation except that extra ethanol and formate were added at various times (indicated by the red arrows). **c)** The same implementation except that extra formate, ethanol, Nox and DERA enzymes were added at various times (indicated by the red arrows). Error bars reflect standard deviations of biological triplicates.

A reaction time course of the optimized system is shown in Fig. 6a. Starting with 140 mM

ethanol, the system produced ~60 mM 1,3-BDO, corresponding to about 85% conversion of

ethanol by day 3. All the ethanol was consumed indicating that ~15% of the ethanol mass

accumulated in intermediates or unidentified side products. In the absence of formate, some 1,3-

BDO production occurred because ADH can utilize NADP+ at a low level. However, if both

formate and NADP$^+$ were removed, we see essentially no production of 1,3-BDO indicating that

the formate-NADPH regeneration system is necessary for effective 1,3-BDO production.

Substrate addition to boost titer:

As 140 mM ethanol was completely consumed in the optimized system, we attempted to further

boost titer by raising the initial ethanol concentration to 350 mM and added new boluses of 88

mM ethanol and 30 mM formate after each day of reaction. As shown in Fig. 6b, 150 mM

ethanol was consumed the first day, generating ~45 mM 1,3-BDO. Ethanol consumption greatly

diminished the next day, however, and almost stopped after two days. While 1,3-BDO

production also slowed (from ~1.8 mM/h to ~0.6 mM/h on day 2 and 3), 1,3-BDO concentrations

continued to rise even in the absence of ethanol consumption, suggesting that intermediates were

more slowly being converted after the initial ethanol consumption.

Enzyme inactivation:

We next sought to learn why the reactions slow down and then stop after several days. It is

possible that the enzymes become inactivated by ethanol or the increasing 1,3-BDO

concentrations. We therefore tested the inactivation of each of the enzymes when challenged

with ethanol or 1,3-BDO in relevant concentration ranges. As shown in Fig. 7, ADH, FDH and

AKR are all stable for several days in both ethanol and 1,3-BDO in the relevant concentration

ranges. DERA is also relatively stable but loses about 20% activity after 2 days in the absence of

solvents. DERA's activity loss is only modestly accelerated by the alcohols, losing ~35% of its

activity in 2% ethanol and ~25% of its activity in 1% BDO. Nox, however, loses ~90% of its

activity after 2 days regardless of solvent conditions. Nox inactivation could therefore explain

the slowing and ultimate cessation of ethanol consumption after several days due to buildup of

NADH, while DERA inactivation is a possible cause of the slow down of 1,3BDO production at

later times.
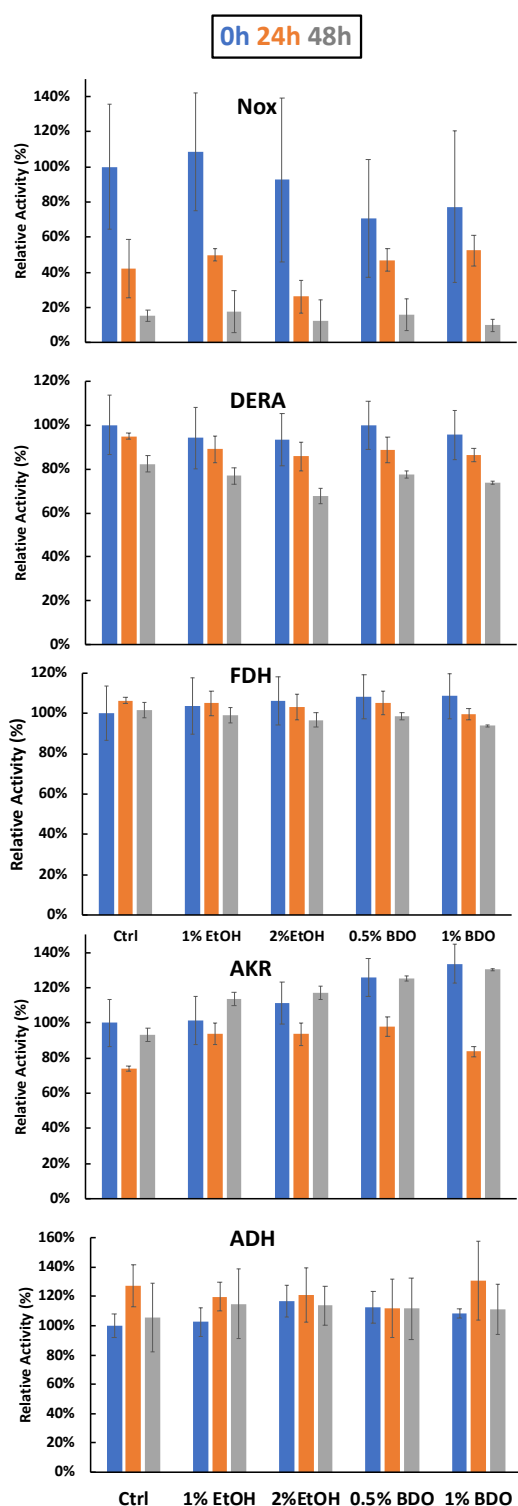
Figure 7. Enzyme inactivation) The activity of the enzymes after 0 (blue bars), 24 (orange bars) and 48 (grey bar) hours of incubation in the absence (Ctrl) or presence of various alcohols as indicated in the horizontal axis. Relative activity refers to the activity as a percentage of the control at 0 hours. Error bars reflect standard deviations of biological triplicates.

Enzyme Replenishment

In an effort to prolong the reactions, we tested additions of fresh Nox and DERA enzymes that are susceptible to inactivation. We repeated the substrate addition experiments while also adding fresh enzyme additions. Starting with 350 mM ethanol, we added 88 mM ethanol and 30 mM formate every 24 hours as before, but also added Nox and DERA enzymes in proportion to their expected loss of activity. With this approach the reactions continued producing

1,3-BDO for 4 days, generating a titer of ~85 mM or 7.7 g/L (Fig. 6c) with an initial productivity

over the first day ~0.16 g/L/h. The final yield was 85% of theoretical in single feed reaction and

54% in the multiday replenishment reaction.

Enzyme specificity and product chirality:

Although the P. aeruginosa AKR employed here was previously identified from an extensive

screen as a highly active and specific for 3-HBal[42], 3-HBal is a chiral molecule and the

stereochemical preference of AKR has not been established. Moreover, while AKR was reported

to have negligible activity with acetaldehyde[42], we noted some ability to reduce acetaldehyde

(Fig. 5b). So we decided to investigate AKR specificity further. We were unable to obtain

stereochemically pure 3-HBal for this investigation, but we were able were able to purchase

stereochemically pure (R) 1,3-BDO, along with the racemic mixture. We therefore decided to

investigate stereochemical specificity using the oxidation reaction from 1,3-BDO to 3-HBal.
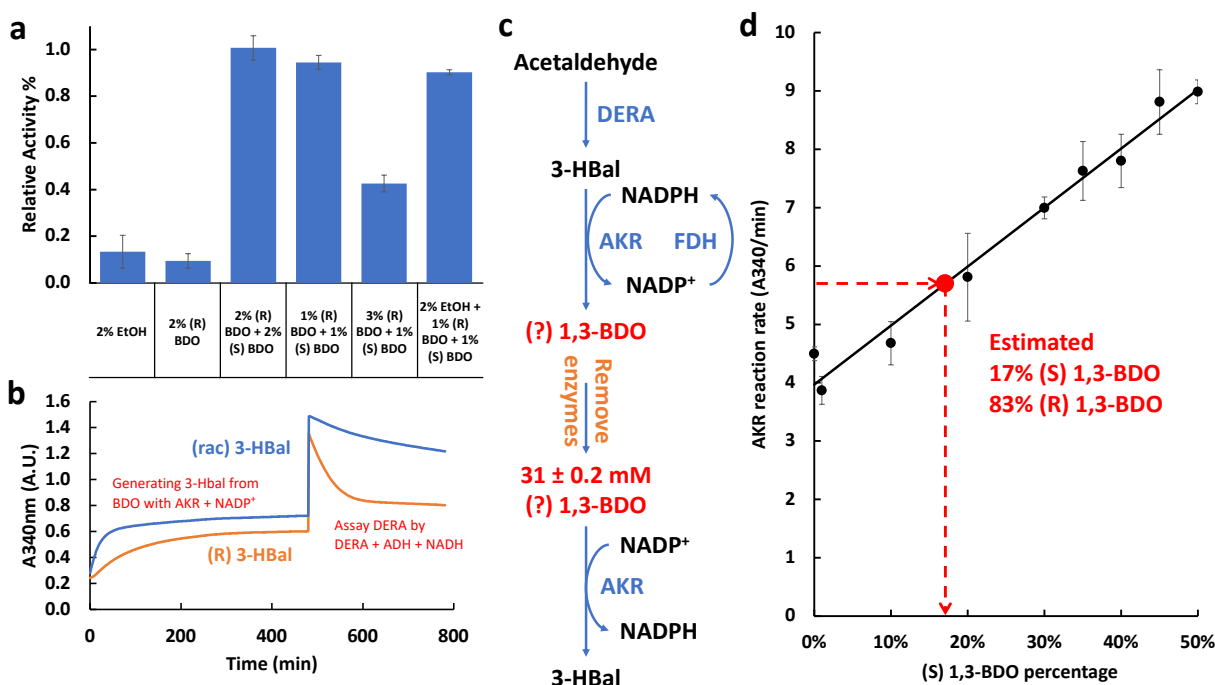
Figure 8. Stereochemical preference of enzymes and product composition. a) Relative AKR reaction rates for oxidation of various alcohols. AKR has a strong preference for (S) 1,3-BDO. Relative activity is the fractional rate compared to 2% (R) + 2% (S) 1,3-BDO. **b)** DERA reaction rates using equal concentrations of the substrates (R) or (R,S) 3-HBal as indicated on the figure. The substrates were generated from 1,3-BDO using AKR and DERA activity measured by a coupled enzyme assay which takes the acetaldehyde product of the DERA reaction and converts it to ethanol with concomitant oxidation of NADH, which is monitored by absorbance at 340 nm. The results indicate that (R) 3-HBal is the preferred substrate. **c)** Scheme for assessing the stereochemical composition of the 1,3-BDO product of the DERA/AKR system. First, the 1,3-BDO product of unknown stereochemical composition was made from acetaldehyde using DERA and AKR enzymes as in the full enzyme system. Then the enzymes were removed and the concentration of the 1,3-BDO was determined (31mM). To assess the stereochemical composition, we then measured the rate of the AKR catalyzed reaction back to 3-HBal. This rate was compared to the rates of the same AKR catalyzed reaction using substrates of known stereochemical composition (panel d). **d)** The standard curve measuring the rate of the AKR catalyzed conversion of 31 mM 1,3-BDO to 3-HBal at different stereochemical compositions. Comparing to the known reaction rates to the rate obtained for the product of converting acetaldehyde to 1,3-BDO using DERA and AKR (red dot), allows us to estimate the stereochemical composition of the product at ~17% (S) 1,3 BDO.

As shown in Fig. 8a, AKR shows similar activity with ethanol and (R) 1,3-BDO, but is about 10-fold more active with the racemic mixture. This result indicates that AKR highly specific for (S)

22

1,3-BDO. Indeed, (R) 1,3-BDO is somewhat inhibitory (compare rates with 1% (S) 1,3-BDO in the presence of 3% and 1% (R)). Our finding that AKR is specific for (S) 1,3-BDO was a surprise because based on the natural reaction, DERA is expected to make (R) 3-HBal and the same AKR used here can make (R) 1,3-BDO in vivo [41]. If so, 1,3-BDO production occurs in spite of a stereochemical mismatch.

To investigate this possibility further, we sought to validate the assumed stereochemical preference of the DERA enzyme for making (R) 3-HBal. To test the stereospecificity of the DERA enzyme, we first used AKR to fully oxidize (R) or (R,S) 1,3-BDO to 3-HBal, thereby generating either (R) 3-HBal or (R,S) 3-HBal. We then assessed DERA activity on the generated substrates. As shown in Fig. 8b, the DERA enzyme is much more active with the (R) substrate than with the mixed substrate, confirming that DERA prefers the (R) stereoisomer. Thus, there is an unexpected stereochemical mismatch between DERA and AKR.

Our results indicate that the DERA enzyme preferentially makes the (R) stereoisomer, but AKR prefers (S). Moreover, AKR has similar activity with (R) 1,3-BDO and ethanol. But this presents a conundrum because the results shown in Fig. 5b reveals that AKR is more reactive with the product of the DERA reaction than with acetaldehyde. To explain this apparent dichotomy, we suspected that DERA must produce at least some (S) 3-HBal along with (R) 3-HBal. If so, then the product would also contain some (S) 1,3-BDO. To test this possibility, we used DERA and AKR to generate 1,3-BDO from acetaldehyde. We then evaluated the chirality of the product by measuring the reaction rate of reverse reaction from 1,3-BDO to 3-HBal and

compared it to the rates of various known ratios of (R) and (S) 1,3-BDO (see scheme in Fig. 8c).

As shown in Fig. 8d, the reaction rate for the 1,3-BDO product suggests that the product indeed

contains ~17% (S) 1,3-BDO.

Discussion

In this work we have taken steps to test and expand ability of cell-free platforms to upgrade

ethanol. Our approach adds flexibility by separating the oxidation of ethanol from the reduction

step required for 1,3-BDO biosynthesis. The production parameters achieved here (0.16 g/L/h

productivity, 7.7 g/L titer and 75-85% yield) are higher than achieved in cells so far (1.1 g/L

titer, <5% yield from glucose) [41], but will clearly require considerable improvement for

commercial viability. Nevertheless, there are obvious avenues for improvement through genome

mining or enzyme engineering. In particular, we discovered a chirality mismatch between the

DERA and AKR enzymes that have been previously developed to make 1,3-BDO in vivo. The

previously identified AKR enzyme prefers (S) 3-HBal, but DERA predominantly makes (R) 3-

HBal. Apparently DERA makes a small amount of (S) 3-HBal and, coupled with the preference

of AKR for (S) 3-HBal, the final product is a mixture of (R) and (S) 1,3-BDO. It should be

possible to improve the rate of the reaction dramatically if the correct chiral substrate could be

delivered to AKR or a different AKR specific for (R) 3-HBal could be identified. Repairing this

mismatch could also be a boon for cell-based production of 1,3-BDO. Another notable issue is

the poor stability of the Nox enzyme in the presence of alcohols. Engineering of finding a more

stable variant could address this problem, however [25]. An advantage of the cell-free approach is

that these issues can be readily identified, making avenues for improvements clear. Ultimately,

we hope that continued efforts to upgrade ethanol using enzyme pathways could provide a path to diversifying current ethanol markets, and ultimately lead to a panoply of carbon negative chemicals in which the carbon is sourced from the atmosphere rather than extraction from the ground.

Chapter 2, Expanding the use of ethanol as a feedstock for cell-free synthetic biochemistry by implementing acetyl-CoA and ATP generating pathways

Hongjiang Liu, Mark Arbing and James U. Bowie*

Department of Chemistry and Biochemistry, Molecular Biology Institute, UCLA-DOE Institute of Genomics and Proteomics, University of California Los Angeles, Los Angeles CA

*to whom correspondence should be address

James U. Bowie

Boyer Hall

611 Charles E. Young Dr. E

Los Angeles, CA 90095-1570

bowie@mbi.ucla.edu

Competing Interests: JUB has co-founded a company, Invizyne Technologies, that seeks to develop cell-free chemical production methods. HL declares no competing interests.

Author Contributions: L.L. and J.U.B. conceived of the project and analyzed results. L.L. performed the bulk of the experiments and M.A. performed some of the cloning required. All the authors contributed to writing the manuscript.

Abstract

Ethanol is a widely available carbon compound that can be increasingly produced with a net negative carbon balance. Carbon-negative ethanol might therefore provide a feedstock for building a wider range of sustainable chemicals. Here we show how ethanol can be converted with a cell free system into acetyl-CoA, a central precursor for myriad biochemicals, and how we can use the energy stored in ethanol to generate ATP, another key molecule important for powering biochemical pathways. The ATP generator produces acetone as a value-added side product. Our ATP generator reached titers of 27 ± 6 mM ATP and 59 ± 15 mM acetone with maximum ATP synthesis rate of 2.8 ± 0.6 mM/hour and acetone of 7.8 ± 0.8 mM/hour. We illustrated how the ATP generating module can power cell-free biochemical pathways by converting mevalonate into isoprenol at a titer of 12.5 ± 0.8 mM and a maximum productivity of 1.0 ± 0.05 mM/hour. These proof-of-principle demonstrations may ultimately find their way to the manufacture of diverse chemicals from ethanol and other simple carbon compounds.

Background

To combat global warming, it is estimated that we need to move to a net carbon negative impact by year 2050[45]. Petroleum forms the basis for most of the chemical compounds used industrially, thereby contributing to greenhouse gas emissions[46]. If these petroleum-based chemicals could be built from carbon recycled from the atmosphere it could greatly reduce our carbon footprint.
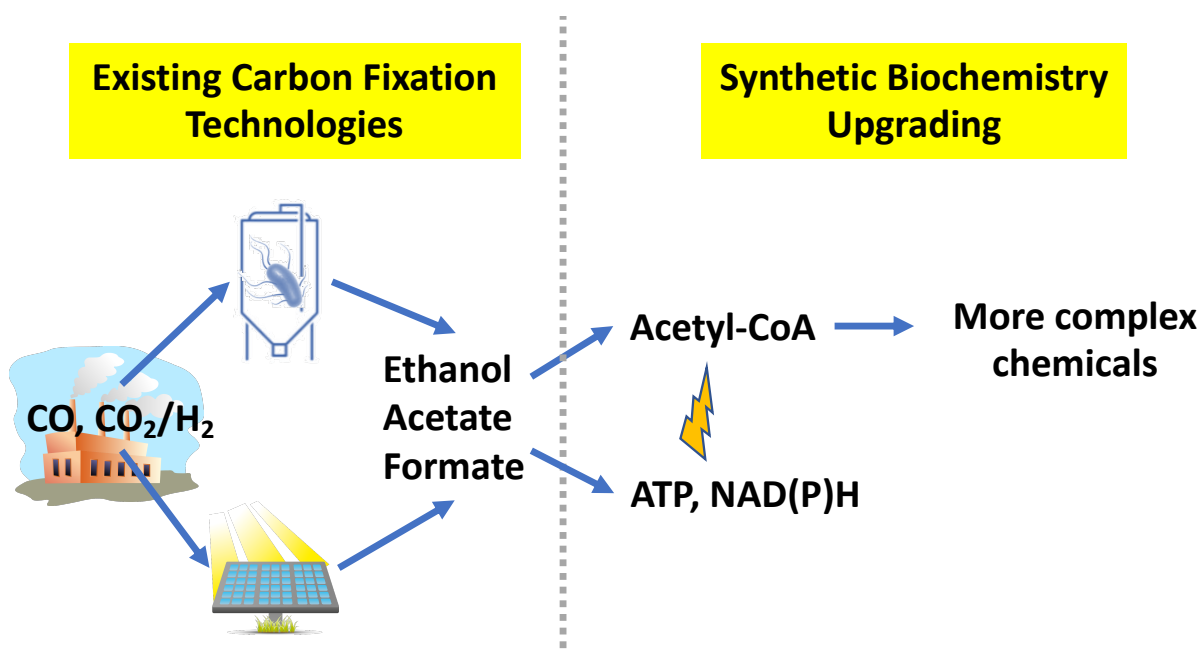
Figure 9. A possible path to a carbon negative chemical industry. Carbon is first fixed from the atmosphere into simple carbon compounds like ethanol and acetate using acetogens or electrochemistry. Cell-free synthetic biochemistry can then be used to make more complex chemicals used directly or as building block carbon chemicals. These building block carbon chemicals could then be used to build still more complex chemicals using existing or new synthetic methods. Key enabling technologies for the application of synthetic biochemistry are methods to generate a central biochemical building block, acetyl-CoA, and the biochemical energy carrier, ATP.

A potential approach for generating diverse carbon-negative chemicals is illustrated in Fig. 9.

The concept starts with simple carbon compounds that can be produced with carbon fixed from

the atmosphere. Advances in microbiology, metabolic engineering and electrochemistry have

made possible the carbon negative production of simple one and two carbon compounds. In

particular, acetogens can efficiently convert flue gas into ethanol and acetate and there are

several commercial plants in development[47–50]. A second development is advances in

electrochemical carbon capture which can convert CO_2 into small carbon compounds like

formate and ethanol with increasing efficiency[51–54]. To the extent that the electrical power is

derived from the sun or nuclear plants, electrochemistry provides another carbon negative

process for making simple carbon compounds. Effective ways to upgrade these simple

molecules into more complex chemicals could therefore potentially form the basis for a carbon

negative chemical industry. To realize this vision of a carbon negative economy, it will be

necessary to develop effective, sustainable methods for converting simple carbon compounds

into more diverse chemicals[55]. The upgraded chemicals could be used directly or employed as

precursors for building additional chemical diversity, thereby replacing myriad petroleum

derived chemicals with carbon negative chemicals.

While it may be possible to use engineered microbes to upgrade simple carbon compounds like

ethanol acetate and formate, an enzymatic cell-free conversion could provide more efficient

methods for complexifying the simple fixed carbon compounds. A cell-free, synthetic

biochemistry approach could potentially provide many advantages over cell-based conversions in

yield, productivity and titers (reviewed in[21]), but will need many advances before it is possible to

employ enzymes on a scale needed for commodity chemical manufacturing. The first step is to

develop pathways that could become viable for cell-free production.

Some initial steps have been made to employ ethanol as a building block chemical for cell-free

synthesis. Zhang et al. developed a system to enzymatically convert ethanol into 2,3-butanediol

and 2-butanol[37]. We developed a simple system for upgrading ethanol into 1,3 butanediol[56]. In

both of these efforts, the pathways run through acetaldehyde which is then fused to make four

carbon molecules. Reducing equivalent power in the form of NAD(P)H is supplied by formate

oxidation. None of these pathways utilize the central biochemical intermediate acetyl-CoA or key energy carrier, ATP.

To increase the diversity of molecules that can be made biochemically from ethanol, it will be important to be able to produce acetyl-CoA from ethanol as acetyl-CoA provides a gateway to myriad biochemical pathways. We also need a way to generate the ATP required for many pathways. Here we show that acetyl-CoA can be generated straightforwardly from ethanol in a cell-free pathway and show how to generate ATP for powering cell-free systems. These pathways add to the toolbox for developing a sustainable chemical industry based on carbon-negative building blocks.

Converting ethanol to acetyl-CoA

Our approach to converting ethanol into acetyl-CoA is shown in Fig. 10a. We first oxidize ethanol to acetaldehyde using alcohol dehydrogenase (ADH) and NAD^+. Acetaldehyde is then converted to acetyl-CoA using aldehyde dehydrogenase (ALDH). The first oxidation step (ADH reaction) is a highly unfavorable thermodynamically[57]. While the second reaction (ALDH reaction) is favorable thermodynamically, the overall reaction is still unfavorable by $+14.5 \pm 2.4$ kJ/mol at a 1 mM standard state[57]. Thus, we need a mechanism to drive the overall reaction forward to produce acetyl-CoA. To accomplish this goal, we introduce an enzyme NADH oxidase (Nox) that re-oxidizes NADH back to NAD^+, which provides a large $\Delta G°$ driving force of -433.5 ± 6.4 KJ/mol. The Nox-catalyzed reaction can thereby maintain a large NAD^+/NADH gradient to drive the conversion of ethanol to acetyl-CoA.
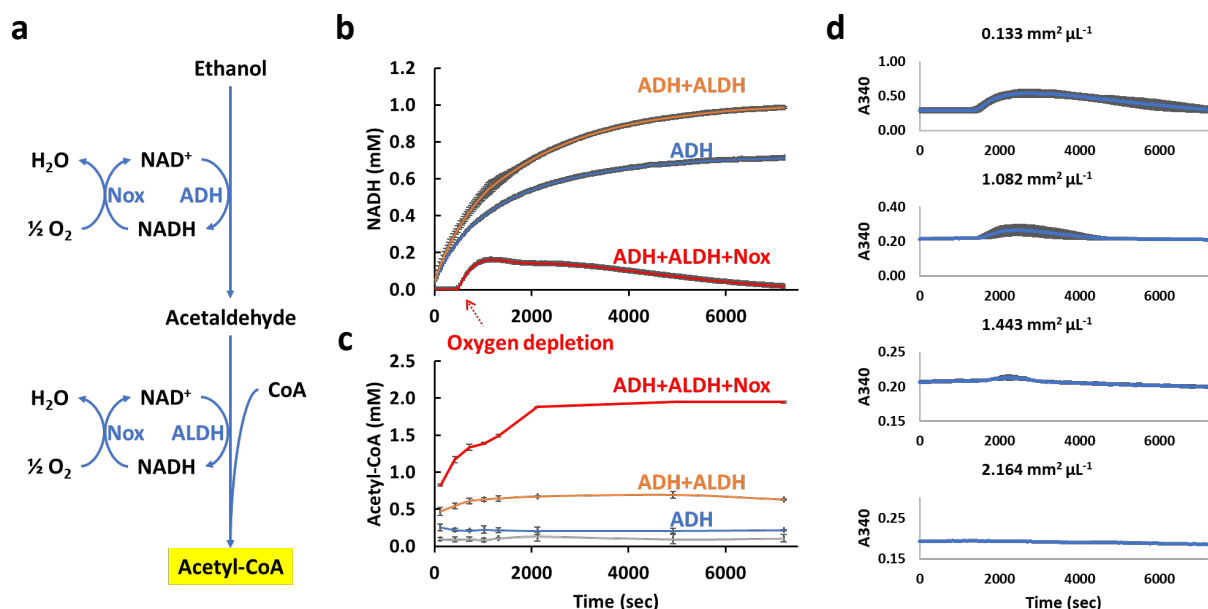
Figure 10. Ethanol to acetyl-CoA module. (a) Schematic of the pathway employed. Reoxidation of NADH, catalyzed by Nox, maintains a concentration gradient to drive the otherwise thermodynamically unfavorable reaction. **(b)** NADH concentration over time with different enzyme combinations as indicated in the figure. **(c)** Acetyl-CoA concentration over time with different enzyme combinations as indicated in the figure. **(d)** The effect of surface area to volume on NADH concentrations over time, using the full system with ADH, ALDH and Nox. All assays experiments were performed in biological triplicates and the error bars reflect the standard deviation.

To test the system for producing acetyl-CoA from ethanol, we built reactions with ADH alone; with ADH and ALDH; and a full system with ADH, ALDH and Nox. We used 2 mM CoA so the maximum possible production of acetyl-CoA would be 2 mM. As shown in Fig. 10b&c, ADH alone (blue traces) oxidizes ethanol, generating NADH as expected, but does not produce acetyl-CoA. However, when ADH was coupled with ALDH (orange traces), the NADH production increased, and some acetyl-CoA was produced. When the full-length acetyl-CoA production module was assembled (red traces), Nox rapidly reoxidized NADH back to NAD^+ (Fig. 10b), allowing acetyl-CoA production up to 1.94 ± 0.01 mM (Fig. 10c), approaching the

theoretical maximum. Thus, we were able to drive the reaction to near completion by the addition of Nox. The acetyl-CoA synthesis rate for the first 2000 seconds was ~3.2 mM h^{-1}

The changes in NADH concentration over time in the full system (ADH, ALDH, Nox) is complex as might be expected for an oxygen dependent reaction. As shown in (Fig. 10b red trace), the NADH concentration is initially undetectable, then increases to a maximum of ~0.1 mM at ~1000 s, then decreases gradually over time. We hypothesize that this behavior was due to oxygen levels in the reaction. In particular, approximately 0.2 mM oxygen is readily dissolved in water under standard state conditions[58]. So, upon production of ~0.2 mM NADH, the dissolved oxygen in solution would be depleted by the activity of Nox. Consistent with this view, the NADH concentration begins to increase after about 0.2 mM NADH is generated (compare to reactions without Nox). At that point the rate of re-oxidation of NADH would be limited by air/water diffusion. To test this hypothesis, we varied the surface area to volume ratio of the reactions by performing the reactions in different sized containers. As shown in Fig. 10d. The NADH concentration rise is more significant at smaller surface:volume ratios and the onset is sooner, while at larger surface:volume, the rise is mitigated. These results suggest that the rate of aeration is indeed a limiting factor after the initial dissolved oxygen is consumed.

An ATP Generating Module to power cell-free synthesis

Economical cell-free systems must employ methods to recycle ATP[59]. It is not viable to simply supply the required ATP due to cost, and the buildup of ADP and phosphate will eventually poison the systems. Recycling can be done by using sacrificial substrates such as creatine

phosphate or polyphosphate, but this approach does not solve the problem of waste product accumulation. Thus, if we want to create cell-free systems that can operate continuously for long periods of time, it is essential to develop ATP generation methods that avoid the buildup of waste products. We therefore wanted to test whether we could use the energy stored in ethanol develop a useful ATP generator for cell-free systems.
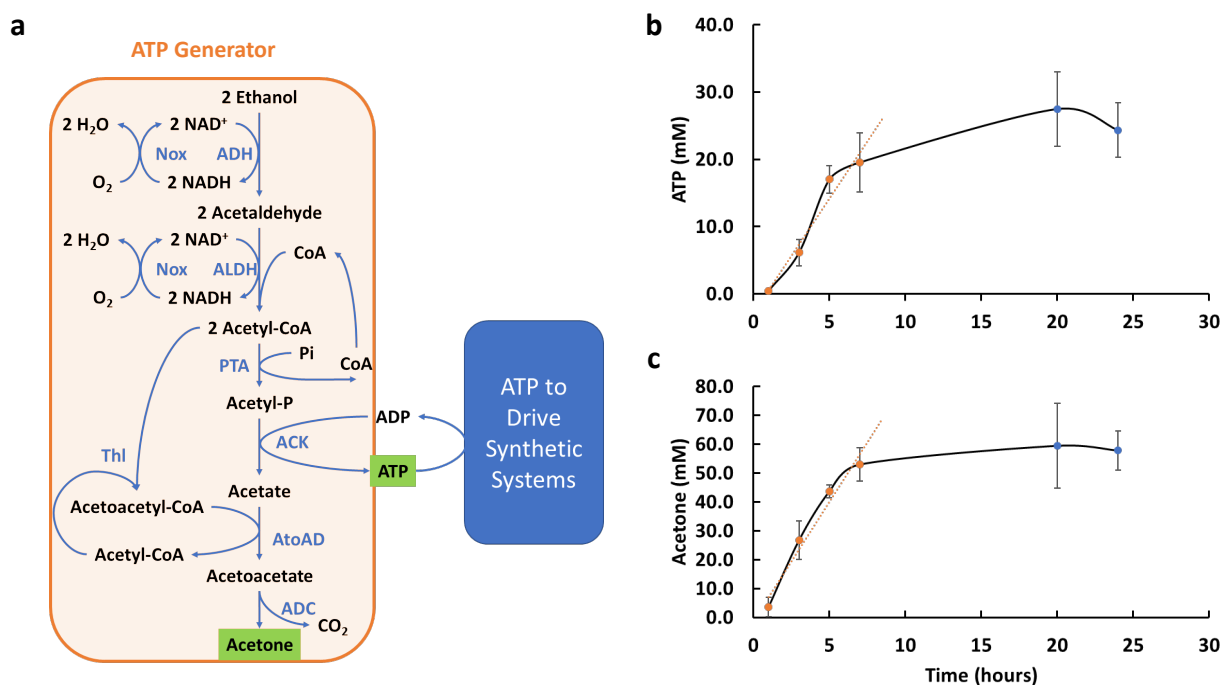
Figure 11. ATP generator module. (a) Schematic of the pathway employed. The input ethanol is converted to acetone, generating ATP in the process. The ATP can then be used separately to drive biochemical pathways. **(b)** The amount of ATP generated over time using the ATP generator module. **(c)** The amount of acetone generated over time using the ATP generator module. All assays experiments were performed in biological triplicates and the error bars reflect the standard deviation.

We designed a potential ATP Generator for the continuous generation of ATP shown in Fig. 11a. The production of acetyl-CoA from ethanol described above enables the production of ATP via the phosphotransacetylase (PTA) and acetate kinase (ACK) pathway. The PTA-ACK pathway

generates the acetate, however, that would ultimately accumulate in the reaction solutions. To deal with the acetate buildup, we added three more enzymes to funnel the carbon into acetone. Acetone is volatile, which provides a means to remove it continuously from the reaction systems by gas stripping. Moreover, acetone is more valuable than ethanol or acetate, providing a value-added side product. To make acetone, we combine two acetyl-CoA to make acetoacetyl-CoA catalyzed by thiolase (Thl). The acetoacetyl moiety can be exchanged with acetate to produce acetyl-CoA and acetoacetate, catalyzed by acetate CoA-transferase (AtoAD). Acetoacetate can then be decarboxylated to acetone and CO_2 via acetoacetate decarboxylase (ADC). The designed system will not only generate ATP for use in other reactions, it adds value by upgrading ethanol to a more valuable product, acetone.

To build the ATP generator, we divided the system up into two parts for testing. First, we wanted to examine our ability to implement ATP generation from ethanol via the PTA-ACK pathway. We therefore truncated the pathway at the ACK step, going from ethanol to acetate (pathway shown in Supplemental Fig. 1a). A seen in Supplemental Fig. 1a the pathway from ethanol to acetate generates ATP (quantified by glucose consumption in a coupled hexokinase reaction). Starting from an initial supply of 1 mM ADP, the minimally optimized system linearly generated/recycled 11.25 ± 0.01 mM ATP over 24 hours, a rate of ~0.46 mM/hr. We next wanted to test our ability to recycle the acetate into acetone, independent of ATP generation. We therefore built a system shown in Supplemental Fig. 2a, to convert ethanol into acetone using exogenously added acetate (rather than acetate generated via ATP production). As shown in Supplemental Fig. 2b, after 24 hours of operation we observed 27 ± 1 mM acetone production

from a system co-fed with ethanol and acetate. These results demonstrate that we had a viable set of enzymes in hand and we were ready to test the full system.

We then set out to build the full ATP Generation Module (Fig. 11). We first assembled the enzymes and cofactors making initial estimations as to appropriate enzyme levels and supplied the system with 2% ethanol (v/v). We then optimized the enzyme levels by either doubling the loading or halving the loading (see Methods for more details) until we saw no significant improvement in ATP and acetone titer in one day reactions. The final time courses of ATP and acetone production for the optimized system are shown in Fig. 12b&c. Both acetone and ATP levels increase rapidly for the first 7 hrs and then plateau, reaching titers of 27 ± 6 mM ATP and 59 ± 15 mM acetone. In the first 7 hrs, the ATP synthesis rate is 2.8 ± 0.6 mM/hour and acetone is 7.8 ± 0.8 mM/hour.

In theory, the amount of ATP produced and the amount of acetone produced should match, but we saw roughly two times as much acetone as ATP. We believe the discrepancy is due to depletion of ATP by contaminating ATPases, perhaps in the form of adenylate kinase that is heat stable and previously found to contaminate cell-free reactions[60]. We assayed for ATPase activity in the enzyme mixture and found that the enzyme mixture indeed contained 1.36 ± 0.008 mM/h ATPase. Efforts to reduce or eliminate ATPase contamination are ongoing, but is a difficult challenge for such a large collection of enzymes. In the current effort, it reduces efficiency of ATP production from ethanol, but does not prevent us from moving forward with testing the use of our ATP generator for powering other biosynthetic systems.

Isoprenol production

Having demonstrated the ability to generate ATP and upcycle acetate waste to acetone, we sought to test the ability of the system to power the ATP-requiring phase of isoprenoid biosynthesis by making isoprenol from mevalonate (MVA). Isoprenoids comprise tens of thousands of molecules, many of which are employed in foods cosmetics, pharmaceuticals [61], and may provide useful biofuels[62]. MVA is being developed as a potential feedstock[63] for high value isoprenoid production or isoprenol can also be used as a precursor for more complex isoprenoid biosynthesis[64–66]. Isoprenol has therefore been a target of metabolic engineering efforts, with Zheng *et al* [67]achieving ~15 mM isoprenol and George *et al* [68] obtaining ~26 mM and Kang *et al*[69] in a semi-scaled batch system obtaining ~125 mM in engineered *E. coli* cells.

Figure 12. Coupling the ATP generator module to power isoprenol biosynthesis from mevalonate. (a) Schematic of the pathway employed. The ATP Generator Module supplies ATP to the two kinases required for the Isoprenol Module. **(b)** The AP amount limits the Isoprenol Module rate. The graph shows the amount of isoprenol produced by the isolated Isoprenol Module overnight as a function of the amount of AP added. To test the Isoprenol Module in isolation, ATP was supplied directly to eliminate the need for the ATP Generator Module. **(c)** Isoprenol production over time by the isolated Isoprenol Module. The AP concentration was set at 7 mg/ml. ATP was supplied to eliminate the need for the ATP Generator Module. **(d)** Optimizing the ratio of optimized ATP Generator Module enzyme concentrations to Isoprenol Module enzyme concentrations. The amount of isoprenol produced by the varying ratios after 5 hours is shown as a measure of initial rate. The best ratio was found to be 1:1. **(e)** Isoprenol production over time using the full system shown in panel **a** and a 1:1 ratio of ATP Generator Module to Isoprenol Module enzymes. All assays experiments were performed in biological triplicates and the error bars reflect the standard deviation.

We designed an Isoprenol Module shown in Fig. 12a (blue box). Inspired by Kang *et al*[70], we decided to construct a minimal three step MVA to isoprenol pathway. First, MVA is phosphorylated by MVA kinase (MVK), consuming 1 ATP. Then through an alternative activity of the ATP-dependent decarboxylase, pyrophosphate mevalonate decarboxylate (PMDC), mevalonate-5-phosphate (M5P) is directly decarboxylated to isoprenol phosphate, with the consumption of a second ATP. PMDC normally decarboxylates mevalonate pyrophosphate[71] but has been shown to also catalyze decarboxylation of the monophosphate (Supplemental Fig. 3)[70]. Finally, the isoprenol phosphate is hydrolyzed to isoprenol via an acid phosphatase (AP). In the designed system, the two ATPs required for the Isoprenol Module are supplied by the ATP Generator Module described above.

We first worked to optimize the Isoprenol Module (MVA to isoprenol conversion) by supplying ATP directly rather than from the ATP Generator Module. From initial guesses at enzyme levels, we varied the enzyme concentration by doubling or halving each enzyme individually and

measured the amount produced after 16 hours (See Supplemental Fig. 4 for details). The only enzyme concentration that significantly affected the titer was the Acid Phosphatase (AP). The other enzymes show minimal effects on titer when either doubled or halved. Hence, we worked to optimize the AP concentration as the AP dominates the total enzyme loading. As shown in Fig. 12b, the amount of isoprenol produced at a fixed time increases with AP concentration even up to 17 mg/ml, although the increase is less dramatic above 7 mg/ml. To keep the total enzyme loading in a reasonable range, however, we decided to fix AP usage at 7 mg/ml. A time course of isoprenol production with the Isoprenol Module alone at 7 mg/ml AP is shown in Fig. 12c. We obtained 7.8 ± 0.2 mM of isoprenol after 24 hours of reaciton. The rate of production in the first 5 hours was ~0.73 mM/h.

Clearly the AP enzyme specific activity will need improvement going forward. To our knowledge, no highly specific and efficient AP has yet been identified for the hydrolysis of isoprenol phosphate[67]. In metabolically engineered *E. coli,* the isoprenol phosphate hydrolysis reaction is apparently catalyzed by several different endogenous phosphatases that need further investigation[67].

With semi-optimized ATP Generator (above) and Isoprenol modules in hand, we sought to put the entire system together (Fig. 12a). A full optimization of 11 enzymes is a major effort that is not warranted at this proof-of-principle stage so we simply varied the concentration of each module as a unit. The enzyme concentrations employed after partial optimization of each module separately we refer to as 1x. The maximum 1x rate we obtained for the ATP Generator

Module was ~2.8 mM/h, while the 1x rate for Isoprenol Module was ~0.73 mM h-1, corresponding to an ATP consumption rate of ~1.4 mM/h. Thus, in theory, the optimal rate should be obtained with a 1:2 ATP Generator Module to Isoprenol Module. As seen in Fig. 12d, we varied the ATP Generator Module enzyme concentrations from 0.2x to 2x relative to the Isoprenol Module enzyme concentrations and measured the amount of isoprenol production after 5 hrs. We found similar titers in a broad range of 0.6: to 1.4:1 module ratios, but the best ratio was 1:1, providing a titer after 5 hours of 4.3 ± 0.1 isoprenol (compared to 3.9 ± 0.5 mM at 0.6:1, near the predicted optimum). We hypothesized that the full system with added enzymes leads to additional ATPase activity so that more ATP needs to be generated than anticipated. Indeed, we found that both the ATP Generator Module and the Isoprenol Module contain substantial ATPase background (the ATP Generator Module enzyme mixture contains 1.36 ± 0.008 mM/h ATPase while Isoprenol Module enzyme mixture contains 0.84 ± 0.02 mM/h ATPase at 1X enzyme concentrations). Given the loading ratio of both components, the addition of the Isoprenol Module will introduce ~47% more ATPase activity, suggesting an explanation for why we needed to run the ATP generator richer than predicted. Using the optimized 1:1 ratio, we monitored isoprenol production over time. As shown in Fig. 12e, the maximum titer is reached after a 24-hour reaction, reaching 12.6 ± 0.8 mM of isoprenol with an estimated maximum rate of production of 8.5 mM/h during the first 5 hours of reaction.

Conclusion

In this work we have demonstrated that it is possible to efficiently convert ethanol to acetyl-CoA, opening up diverse avenues for upgrading ethanol to more complex molecules. As one

application we upgraded ethanol to more valuable acetone via an acetyl-CoA intermediate. We also demonstrated a method for transferring the energy in ethanol into the biologically versatile ATP molecule, with an acetone side product. Acetone is volatile and can therefore be readily extracted continuously, so the pathway can provide a way to provide ATP power to cell free systems without building up waste products. Unlike traditional ATP recycle methods that rely on sacrificial substrates such as polyphosphate or creatine phosphate, the pathway avoids buildup of phosphate waste [59]. In this case, our ATP generator can recycle somewhere between 27 ± 6 mM ATP to 59 ± 15 mM ATP in 24 hours of operation. We implemented a simple application of this concept by using the ATP Generator Module to drive the production of isoprenol from mevalonate.

The pathways described here expands the potential use of ethanol as a feedstock molecule for the generation of carbon negative chemicals. Clearly much work is needed for practical use of these pathways, however. Most notably, the ATP Generator Module will need to operate sustainably for much longer periods of time. We have not investigated why ATP generation stops, but enzyme stability is a common cause of reaction cessation in cell-free systems[56,72]. Improving stability will be a critical element of further optimization. ATPases are common contaminants that complicate the setup of cell free systems and reduce efficiency. Extensive purification to remove ATPases will not be tractable for large scale cell-free manufacturing, so we need to develop simple methods for removing ATPase contamination. For example, the Honda group developed an *E. coli* strain with a temperature sensitive adenylate kinase, allowing elimination of adenylate kinase activity by a simple heat treatment[60]. A similar approach may be effective for

removing other ATPases in *E. coli* extracts. Another major factor that will require additional

developments is cofactor costs. We will need to develop methods for making cofactors more

cheaply or employ cheaper cofactor analogs[73–75]. CoA is particular problematic in this regard so

lowering CoA costs would be important enabling technology for cell-free manufacturing and

therefore should be a focus of research in cell-free systems[60].

Future Directions
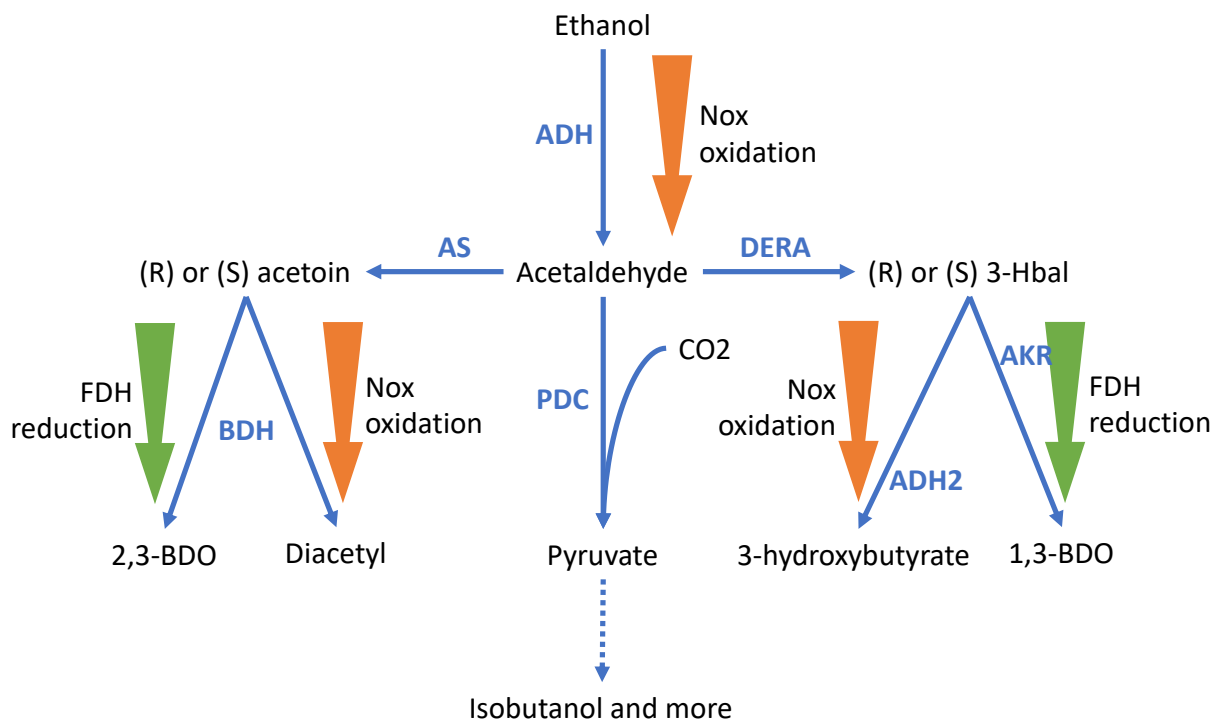
Figure 13) For the aldehyde system, it is possible to lead three distinct product types immediately with proper enzyme discoveries. 2,3-BDO and 1,3-BDO representing the reductive-type products and diacetyl or 3-hydroxybutyrate are the oxidative-type and lastly by further incorporating CO_2, more complex alcohol such as isobutanol can be produced.

This thesis study naturally leads to the expansion of ethanol upgrade platforms. In fact, 1,3-BDO is only a fraction of the proposed bigger picture. By using different enzymes, it is well within the realm of possibility to build other interesting industrially relevant products. Towards building more diversified products and optimizing the 1,3BDO pathway, I, Dr. Jim Bowie and Invizyne have been awarded an ARPAe grant for ECOSynBio[76] and through this collaboration, we will continue to explore the proposed work in the above illustration.

In this proposed plan, we should be able to produce four very interesting commodities (see in figure 13), first, by directing acetaldehyde either through DERA as introduced in chapter two of this dissertation, or yet to be optimized acetoin synthase (AS), we can get to either acetoin or 3-hydroxybutanal (3-Hbal). Then, by using either AKR as shown in chapter two, or potentially using some engineered or natural homologs of butanol dehydrogenase (BDH) together with FDH, we can drive the reduction to either 1,3-BDO and 2,3-BDO, which both are interesting fuel candidates and can be further processed to respective butadienes. Butadienes are used in vast quantities and the ability to replace petroleum-derived butadiene could have large impact on CO_2 emission reduction. Alternatively, through oxidation with engineered BDH or ADH along with Nox providing the driving force as shown in chapter one and two, we can potentially make diacetyl or 3-
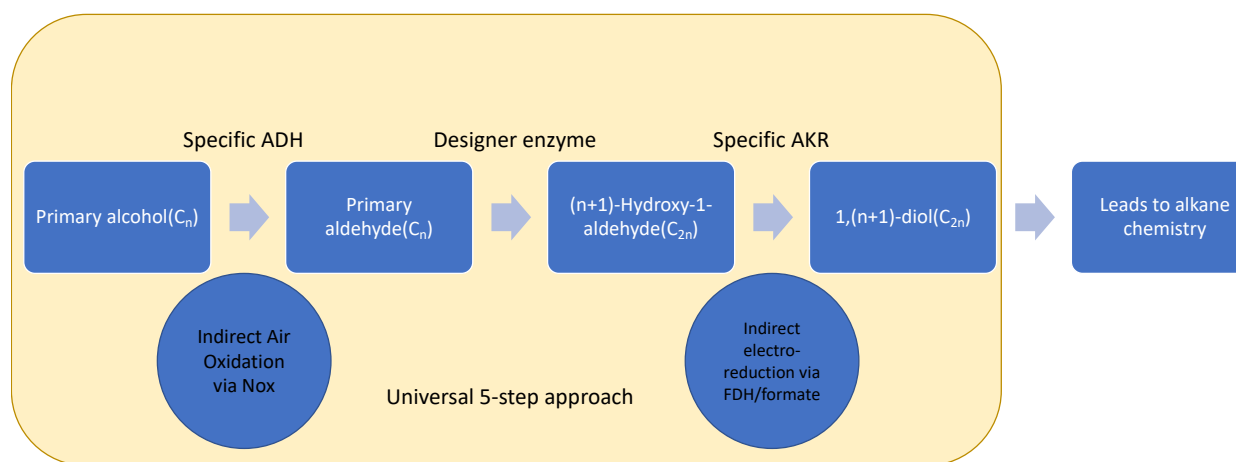

Figure 14) Possible blueprint to build any C_{2n} diol type alcohols with proper designer DERA enzymes.

hydroxybutyrate. Diacetyl is an important food flavoring agent and represents a potential route of commercialization. 3-hydroxybutyrate is an interesting precursor to proposed polyhydroxyalkanoate (PHA) bioplastics. PHA bioplastics could potentially bring another large

43

amount environmental improvement. Lastly, pyruvate is the core of central metabolism, and any more applications will be developed based on pyruvate enabled chemistries. The most notable example is the production of isobutanol, a promising fuel with high energy density of low water content, which are paramount to engine adoption.

Also, as shown in illustration 14, with designer DERA and AKR enzymes, it is possible to build any combinations of diols and ultimately lead to a panoply of carbon negative chemicals in which the carbon is sourced from the atmosphere rather than extraction from the ground. The key challenge lies in enzyme engineering and upstream resource availability of different alcohols. Much of the DERA and AKR reaction will likely require designer enzymes engineered to accept unnatural substrates. While the prospects are certainly interesting, the engineering could become a long arduous journey. This is a risk factor of any bio-based or bio-inspired chemical production.
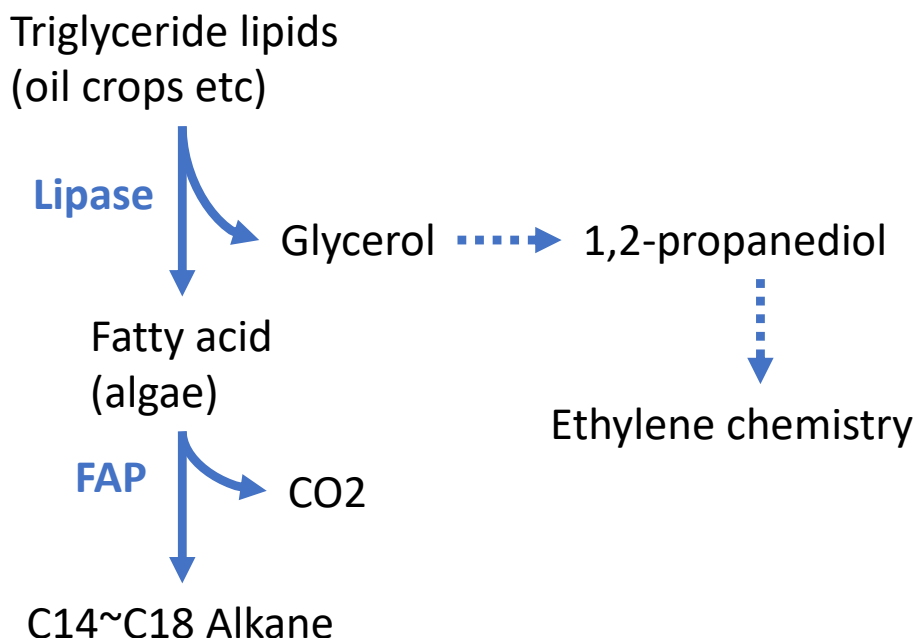
Figure 15) Possible blueprint to build long alkanes from bio-oils.

Lastly, I also will expand the field of synthetic biochemistry as a platform to connect upstream biological processes and downstream chemical processes. One key link I identified is the field of biodiesel production. Historically, many biological platforms are focused on producing long chain free fatty acid (FFA). However, these free fatty acids are incredibly difficult to accumulate in most of the host organisms due to severe competition with the endogenous pathways and inherent toxicity to the cell (largely by disrupting cell membranes). Also, lipids or FFAs are still not ideal for the modern petrochemical industries and engine designs. However, many experimental organisms can already produce oil and fat (i.e., triglyceride lipids) very well, and the efficiency is only a matter of incremental improvement and will increase in the future such as the work done in NREL[6]. Hence, by designing a platform as shown in figure 15, I should be able to alleviate the production issues of FFA by using stabilized enzymes and directly produce long

chain alkenes efficiently. First through lipase, triglycerides can be broken into glycerol and FFA. Then, thanks to recent discoveries and development of Fatty Acid Decarboxylase (FAP)[77], we should be able to one-step decarboxylate the terminal carboxyl group and produce pure alkane. Lastly, these C14 to C18 alkenes are already highly demanded commodities in the modern petrochemical industries.

It should also be noted that algae systems are decent in producing FFA[78], which we can directly use to produce free alkanes with a one enzyme cell-free system. However, currently the algal biofuel progress is limited to four bottlenecks[79]. Firstly, algal biofuel production is limited to the hardiness of the algae towards oil accumulation and the adverse growth environment. Secondly, it is limited to the access of sufficient CO2 in the growth condition. Thirdly, its it limited to access of sufficient sunlight to grow in very high density. Lastly, the extraordinary water and space usage of farming algae is costly to scale. I do expect these challenges to be eventually addressed. Hence upgrading algae oil into alkane products still poses an interesting future once upstream hurdles can be solved in time.

To be able to compete with natural fossil oil resources commercially, my platforms need to be extremely optimized, the path to such optimization is attainable and I think this is the path that will lead to the significant amount of carbon emission reduction in a future carbon negative biobased economy.

Methods

Molecular Cloning

All genes except AtoAD were codon optimized for *E. coli* using Twist Biosciences online suite (For DNA sequences please see Supplemental Information). All genes except AtoAD were synthesized and cloned by Twist Bioscience into the Nde1-Xho1 site of pET28b plasmid. The ADC clone was further manipulated to remove the N-terminal HisTag. The AtoAD complex is encoded within the genome of *E. coli* DH5α by a bicistronic operon in which the stop codon of AtoD overlaps with the start codon of the AtoA gene. The AtoAD bicistron was PCR amplified from *E. coli* DH5α genomic DNA using the primers 5'-AACCTGTATTTCCAGAGTATGAAAACAAAATTGATGACATTAC-3'and 5'-GTGATGGTGATGGTGATGAGTTAAATCACCCCGTTGCGTATTC-3'. The PCR product was purified and cloned, by Gibson Assembly, into the pMAPLe3 expression vector[80] which appends a hexahistidine tag to the C-terminus of the gene product (AtoA). Sequences were verified (Genwiz) and used to transform *E. coli* Bl21 (DE3) Gold and individual colonies selected. The transformed strains were stored frozen in culture medium with 30% glycerol at –80 °C. For expression, all plasmids were transformed into E. coli Bl21 (DE3) Gold except for FDH which was transformed into E. coli C43.

Protein expression and purification

For enzyme production and purification, frozen stocks were used to inoculate 1 L auto-induction media containing 50 mg/L kanamycin. The auto-induction media was prepared by adding 0.5 g glucose and 2 g lactose mixture into Miller's formula Luria-Bertani medium and then autoclaved

for 30 min. The cells were grown for approximately 20 hours at 37°C and the cells collected by centrifugation at 3720 x g for 30 min. The cell pellets were resuspended and incubated in 20 mL Hypotonic Thermolysis Buffer (50 mM NaCl, 20 mM Tris-HCl pH 7.5) with 2.5 mg chicken egg-white lysozyme (Sigma-Aldrich) for 10 min. Then, the resuspensions (except AtoAD and Nox) were heated to 60°C for 30 min. FDH was expressed by growing cells at 37 °C to OD600 ~0.8 in LB medium with 50 µg/ml kanamycin, induction with 1 mM IPTG and incubation overnight at 18 °C. AtoAD and Nox are not thermostable, FDH, AtoAD and Nox suspensions were lysed with an Emulsiflex homogenizer at 10000 bars, substituting for the heat step. All the cell lysates were then incubated with 2500 units benzonase nuclease (Sigma-Aldrich) and centrifuged at 24,465 xg for 30 min.

The resulting clear supernatants were further processed by Ni-NTA chromatography (except ADC, which did not have a 6xHis tag). First, the clear lysates were incubated with 3 mL (bed volume) of Ni-NTA (Qiagen Superflow) for 30 min at 4°C. Then, the resulting mixtures were transferred to a gravity flow column and washed with 2x 10 mL Hypotonic Thermolysis Buffer followed by 2x 10 mL Wash Buffer (300 mM NaCl, 50 mM Tris-HCl pH 7.5, 5 mM imidazole). After washing, the enzymes bound to the Ni-NTA bed were eluted with Elution Buffer (150 mM NaCl, 50 mM Tris-HCl pH 7.5, 250mM imidazole, 10% glycerol).

For the tagless ADC, a clear, heat-treated lysate was prepared as described above, and then concentrated with a 30 KD cutoff concentrator (Millipore Amicron Ultra) to below 5 mL. The

concentrated lysate was then dialyzed into Storage Buffer (150 NaCl, 50 mM Tris-HCl pH=7.5 and 10% glycerol).

Protein concentrations were measured by absorbance at 280nm and purity evaluated SDS-PAGE. Visually, the purified Nox enzyme was brilliantly yellow, while the rest were colorless. For long term storage, all enzymes were flash-frozen in Elution Buffer with liquid nitrogen and stored in -80°C.

Gas-Chromatography

For GC-MS, 1 μL of sample from the respective organic phases were injected automatically with an autosampler system, in split-less mode. Ultrapure helium was used as carrier with the flow set to 30 mL min^{-1} in constant flow mode. Separation was carried out on a Thermo-Scientific TG-WAXMS column with dimensions of 30 m x 320 μm x 0.25 μm. The Flame Ionization Detector was ignited with 350 mL min^{-1} ultrapure air and 35 mL min^{-1} hydrogen at constant flow. Data was recorded with Chromeleon 7 software.

For BDO detection, the initial oven temperature was set to 50 °C for 2 minutes followed by a 10 °C min^{-1} ramp to 140 °C, then a second temperature ramp of 50 °C min^{-1} to a final temperature of 235 °C, which was maintained for 3 min. Both inlet and detector temperatures were set at 250 °C.

For acetone detection, the initial oven temperature was set to 35 °C for 2 minutes followed by a 10 °C min^{-1} ramp to 140°C, then a second temperature ramp of 50 °C min-1 to a final temperature of 235 °C, which was maintained for 3 min. The Flame Ionization Detector was set at 250 °C.

For isoprenol detection, the initial oven temperature was set to 50 °C for 2 minutes followed by a 50 °C min^{-1} ramp to 80°C, then a 5 °C min^{-1} ramp to 125°C, then a ramp of 50 °C min^{-1} to a final temperature of 235 °C, which was then maintained for 3 min. The Flame Ionization Detector was set at 250 °C.

Ethanol oxidation module

Reactions were performed in 2 mM NAD$^+$ and 100 mM ethanol in the General Buffer (10 mM KCl, 50 mM NaCl, 10 mM MgCl2 and 100 mM Tris-HCl, pH 7.5). 100 µl reactions were initiated by adding ADH to a final concentration of 0.01 mg/mL, or a mixture of ADH or Nox at final concentrations of 0.01 mg/mL and 0.08 mg/mL, respectively. The reaction was monitored by absorbance at 340 nm, recorded in a SpectraMax M35 plate reader. Acetaldehyde was directly assayed using a purpald assay. 10 µL of the reaction mixtures were added to 90 µL of purpald reagent (5 g/L purpald in 0.5 M NaOH). After incubation at room temperature for 10 min, the absorbance at 550 nm was measured. Acetaldehyde concentrations were determined by comparison to a standard curve developed using known concentrations of acetaldehyde.

Reductive module and substrate specificity

The reactions consisted of 50 mM acetaldehyde and 2 mM NADPH in the General Buffer.

Reactions were initiated by the addition of 0.1 mg/mL (final) AKR with or without 1.5 mg/mL

(final) DERA and the reactions monitored by absorbance at 340 nm.

1,3-BDO production

Optimized single batch BDO production consisted of the following mixture in General Buffer: 1

mM of NADP$^+$, 4 mM of NAD$^+$, 140 mM ethanol, 50 mM formate (pH = 7.4) and enzymes (0.13

g/L of ADH. 0.51 g/L of Nox, 3 g/L of DERA, 0.28 g/L of AKR and 0.29 g/L of FDH). 200 µl

solutions were placed in 12 mL threaded glass tubes and the tubes were sealed tight and

incubated at 29   C with mixing on a rotating drum. The reactions were stopped at various

timepoints by freezing at –80   C. After the vessels were brought to room temperature together,

the reactions were extracted with 200 µL 1-hexanol by vigorous mixing followed by

centrifugation. The organic phase was collected for analysis by GC-FID (Thermo Scientific

TRACE 1310 GC) or GC-MS (Agilent 6890 Gas Chromatograph, and 5975 Inert Mass Selective

Detector) as described below. The titer was determined by comparison to a calibration curve of

analytical 1,3-BDO prepared in similar manner.

The optimized reactions with replenishment were initiated in the same manner as the optimized

single batch BDO production as described above. Every 24 hours the reactions were replenished

by the addition of fresh air, 88 mM ethanol, 50 mM formate pH = 7.4, 0.27 g/L Nox and 0.75 g/L

DERA (total replenishment volume of 13 μL). Then the tubes were resealed and incubation continued. Reactions were processed as described above.

Stereochemical assessment assays

AKR assays employed 0.18 mg/mL AKR and 2 mM $NADP^+$ in General Buffer. Reactions were initiated by the addition of ethanol, R-1,3-butanediol or rac-1,3-butanediol and the reactions monitored by absorbance at 340 nm to obtain initial rates.

To assess DERA stereospecificity we first generated (R) or (R/S) 3-HBal from 1,3-BDO using AKR. We oxidized 1% 1,3-BDO to 3-HBal in General Buffer using 0.18 mg/mL AKR and 1 mM $NADP^+$ for about 8 hours. We then assessed DERA activity on the 3-HBal product by adding 1.6 mg/mL DERA and 0.21 mg/mL ADH and 1 mM NADH. In this reaction, DERA catalyzes the conversion of the 3-HBal product to acetaldehyde, which is then conveniently monitored by conversion to ethanol.

To assay the stereochemical composition of the 1,3-BDO produced by the combination of DERA and AKR, we produced 1,3-BDO using 100 mM acetaldehyde as feedstock with 50 mM formate and 1 mM $NADP^+$ to drive the reductive phase for 24 hours. The enzyme loading was same as in the optimized system. After the reaction was complete, enzymes were removed by passage through a 3 KDa cut-off membrane (Amicon® Ultra-15 3KDa). The flow-through was collected and 1,3-BDO concentration measured to be 31 mM using the GC-FID as described above. We then measured the rate of AKR oxidation of the product back to 3-HBal by adding 0.18 mg/mL

AKR and 5 mM NADP+, monitoring NADPH production by absorbance at 340 nm. The rate was compared to the rate obtained for a series of standards with known stereochemical mixtures.at the same 1,3-BDO concentration as the product (31 mM).

Ethanol oxidation to acetyl-CoA

To set up the testing reactions, 1 mM NAD$^+$, 1 mM CoA and 100 mM ethanol were mixed in General Buffer (GB, consists of 10 mM KCl, 50 mM NaCl, 10 mM MgCl2 and 100 mM Tris-HCl buffer at pH 7.5). Different enzymes combinations were added to start the reaction: (1) 0.01 mg/mL ADH; (2) 0.01 mg/ml ADH plus 0.02 mg/mL ALDH or (3) 0.01 mg/ml ADH, 0.02 mg/mL ALDH and 0.08 mg/mL Nox at a final reaction volume of 200 µL. 340nm absorbance (A340) changes were recorded with a Molecular Device SpectraMax M5 96-well plate reader.

Acetyl-CoA concentrations were measured by a free-thiol assay using Ellman's Reagent (5,5-dithio-bis-(2-nitrobenzoic acid), DTNB). First, a fresh Ellman's stock reagent was made containing 1 mg/mL of DTNB in Ellman's Buffer (1 mM EDTA and 100 mM sodium phosphate at pH 8). The free-thiol measurements were performed by mixing 50 µL samples with 10 µL Ellman's reagent and 140 µL Ellman's Buffer. Following incubation at room temperature for 15 min, the absorbance at 412 nm was measured and compared to a calibration curve. The calibration curve was prepared using authentic trilithium CoA (Sigma-Aldrich).

To observe the relationship between oxygen availability and NADH levels, the same ADH+ALDH+Nox reactions were set up in various multiwell plates with distinct surface to volume ratios plates.

Acetone production and ATP production

To test acetone production with ethanol and acetate as co-feed we used 4 mM of NAD$^+$, 4 mM CoA, 1% ethanol and 50 mM acetate (pH 7.4) in GB. To start the reaction, an enzyme mixture was added to final concentrations of 0.13 g/L of ADH, 0.85 g/L of ALDH, 0.51 g/L of Nox, 0.21 g/L of Thl, 0.5 g/L of AtoAD and 2.65 g/L of ADC. The final reaction volume was 200 μL. To ensure sufficient oxygen while preserving the volatile components, the reactions were performed in 12 ml glass screw top vials. The reactions were performed at 37°C and incubated the same manner as before. After reaction, the solutions were brought back to room temperature and 400 μL of phenetole was quickly added to the reaction. The mixture was then transferred to solvent resistant centrifuge tubes and vigorously vortexed and spun down in a centrifuge. The organic phase was collected for Gas-Chromatography with Flame Ionization Detection (GC-FID) with a Fisher Scientific Trace 1310 system. The titer was extrapolated from a standard curve of analytical acetone that has been treated the same way with enzyme reaction in buffer and shaking.

To test ATP production with ethanol as the sole-feed we used 4 mM of NAD$^+$, 4 mM CoA, 1 mM ADP, 20 mM Na-Pi (pH 7.4), 1% ethanol and 50 mM Glucose in GB. To start the reactions a mixture of enzymes was added to final concentrations of 0.13 g/L of ADH, 0.85 g/L of ALDH,

0.51 g/L of Nox, 0.21 g/L of Thl, 0.14 g/L of PTA, 0.045 g/L of ACK and 0.2 g/L of hexokinase. The final volume was 200 μl. The reactions were measured individually at various time points ranging from 1 to 24 hours. To measure ATP generation, we utilized a reporter platform by converting glucose and ATP to glucose-1-phosphate through hexokinase. This single step reaction recycles ADP/ATP while consuming free reducing sugar. The amount of remaining free reducing sugar can be measured with a glucose assay (adapted from Sigma-Aldrich). Simply, Glucose Assay Buffer was freshly prepared, consisting of 60 mM potassium phosphate (pH 5.9), 0.012% 4-amino-antipyrine, 0.024% N-Ethyl-N-(2-hydroxy-3-sulfopropyl)-m-toluidine (EHSPT), 0.012 mM FAD, 1.2 mM EDTA, 16 mM MgCl2, trace amount of peroxidase (Goldbio) and glucose oxidase (Calbiochem). The assay mixture was made fresh each time before use and the glucose calibration curve was plotted freshly along with a new mixture right before use. 5 μL of assay samples were mixed with 95 μL freshly made Glucose Assay Buffer, incubated at 37°C for 30 min and the absorbance 550 nm measured. The absorbance response was then compared to a standard curve prepared with glucose.

For the reactions combining ATP production and acetone production into a continuous co-production process we used 4 mM of NAD^+, 4 mM CoA, 1 mM ADP, 20 mM sodium phosphate (pH 7.4), 1% ethanol and 50 mM Glucose in GB. To start the reactions, an enzyme mixture was added to make final concentrations of 0.13 g/L of ADH, 0.85 g/L of ALDH, 0.51 g/L of Nox, 0.44 g/L of Thl, 0.14 g/L of PTA, 0.045 g/L of ACK, 0.5 g/L of AtoAD and 2.65 g/L of ADC and 0.2 g/L of hexokinase. Then the samples were individually measured at various time points

with both the Glucose Assay to measure ATP regeneration and by GC-FID to measure acetone co-production as described above.

ATP Acetone Co-production Optimization

To optimize the performance of ATP production, we either doubled or halved all components in the co-production scheme in every round of optimization. The best outcome conditions were combined to initiate the next round of optimization. This approach was repeated 3 times. The best conditions found were as follows: 4 mM of NAD^+, 4 mM CoA, 1 mM ADP, 20 mM sodium phosphate (pH 7.4), 1% ethanol and 50 mM Glucose, 0.38 g/L of ADH, 0.85 g/L of ALDH, 0.51 g/L of Nox, 0.22 g/L of Thl, 0.14 g/L of PTA, 0.045 g/L of ACK, 0.25 g/L of AtoAD and 1.5 g/L of ADC and 0.2 g/L of hexokinase in GB.

Isoprenol Module Optimization

To optimize the performance of MVA to isoprenol production, the MVA, PMDC, and Acid Phosphatase (MP Biomedicals) were either doubled or halved (high and low conditions). After determining that the rate was limited by the AP concentration, AP usage was gradually increased from 0.5 g/L to 17.5 g/L. Considering the large enzyme load and volume constraints, we set the AP level at 7 g/L acid. Since the total enzyme loading is so dominated by the AP concentration, we did not further adjust the MVA and PMDC concentrations. The final enzyme concentrations considered to be broadly optimized were: 0.1 g/L MVK, 0.4 g/L PMDC and 7 g/L Acid Phosphatase.

Full System Optimization

To optimize the full-length system, the system was divided into two sub-systems: the ATP Generator Module and the Isoprenol Module. Using the optimized concentrations described above, we define a 1:1 ratio as one part of the optimized isoprenol module to one part of the optimized ATP module. We tested the mixture with ratios of the ATP Genenerator Module to Isoprenol Module ranging from 0.2 to 2.0 with the total volume fixed. All reactions were allowed to run for 5 hours to obtain a rough estimation of initial rates, and assayed for isoprenol levels on GC-FID. The best condition is as follows: 4 mM NAD^+ , 4 mM CoA, 4 mM ADP, 20 mM sodium phosphate (pH 7.4), 2% ethanol, 0.38 g/L of ADH, 0.85 g/L of ALDH, 0.51 g/L of Nox, 0.22 g/L of Thl, 0.14 g/L of PTA, 0.045 g/L of ACK, 0.25 g/L of AtoAD and 0.5 g/L of ADC, 0.1 g/L MVK, 0.4 g/L PMDC, 7 g/L Acid Phosphatase, buffered in 1x General Buffer.

The reactions were performed in sealed glass containers (200uL total volume in 12 mL glass tube) and then incubated at 37°C with rotation at 60 rpm. After the reaction, the vessel was brought to room temperature, 1x volume of hexane was quickly added then the mixture was transferred to solvent resistant centrifuge tubes. The mixture was then vigorously vortexed and centrifuged, and the organic phase was collected for GC-FID.

ATPase contamination assay

To assay background ATPase activity, we used a coupled pyruvate kinase (PK) lactate dehydrogenase (LDH) assay. 5 µL of each enzyme was co-incubated with PK/LDH assay mix. A master mix was made fresh containing 3 mM NADH, 3 mM ATP, 3 mM

phosphoenolpyruvate, and 3 μL PK/LDH mixture per 195 ul total (Sigma-Aldrich P0294)

buffered in General Buffer. To assay enzymes, 5 μL of enzyme sample was mixed with 195 μL

master mix. In the presence of ATPase, ATP is hydrolyzed to ADP, triggering the PK/LDH

reaction to consume NADH, which can be conveniently monitored by absorbance at 340nm.

Nox was not included in these assays since it directly consumes NADH.

Supplemental Information
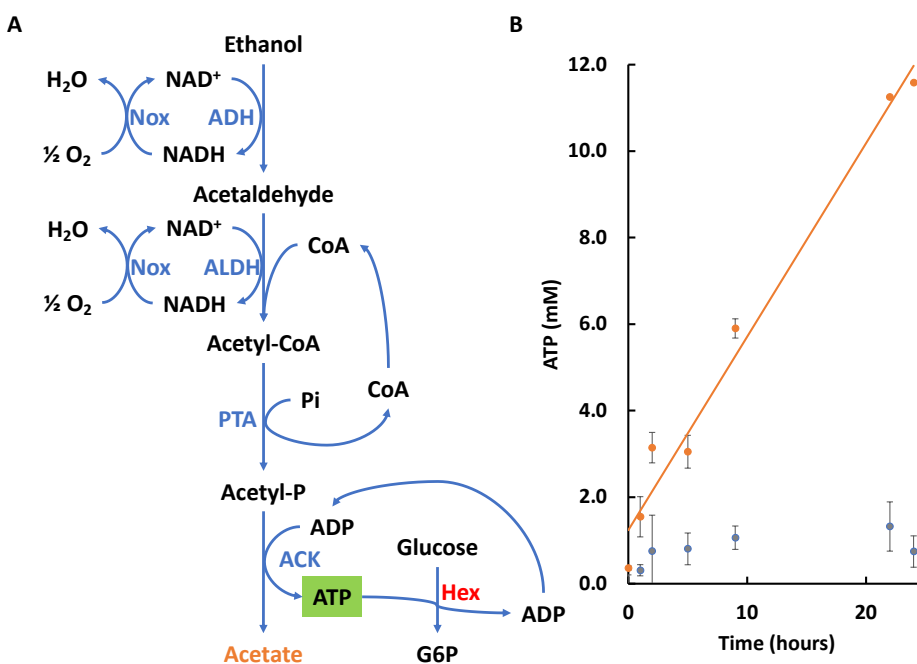
Supplemental Figure 1. Verification of ATP generation, A) scheme of
the partial system to verify continuous ATP generation via acyl-transfer
reaction, **B)** ATP generation measured via hexokinase.
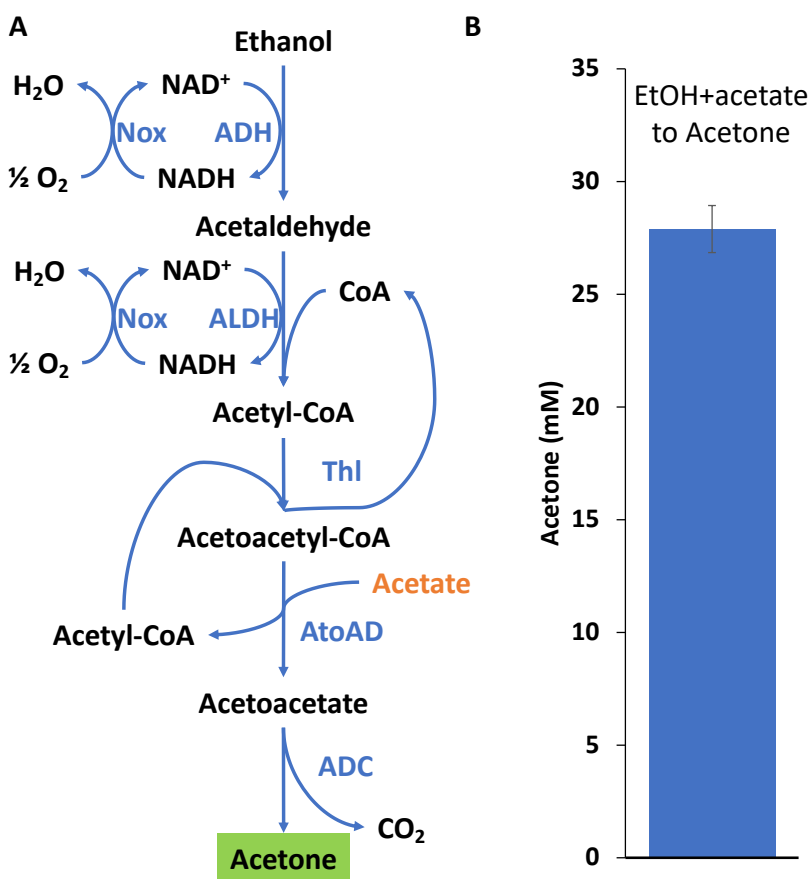
Supplemental Figure 2. Verification of acetate upcycling, A) scheme of the partial system to verify acetate upcycling, **B)** acetone production from ethanol acetate co-feeding.
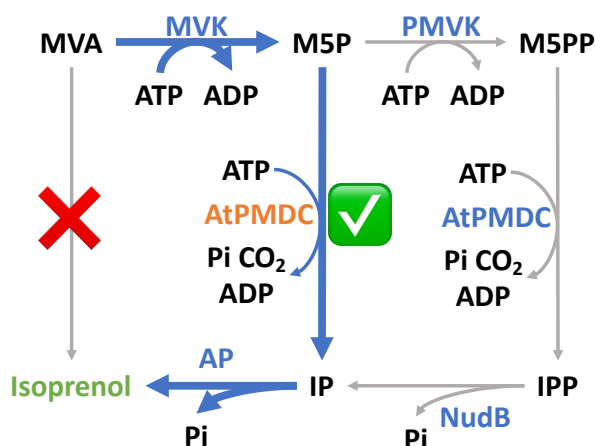
Supplemental figure 3. Schematic of possible Mevalonic acid to isoprenol modules), three distinct paths are possible to go from MVA to isoprenol.

There are multiple pathways for converting MVA into isoprenol. The natural biosynthetic pathways all converge on isopentenyl pyrophosphate. In theory, MVA could be directly decarboxylated to isoprenol, but no enzyme is known to catalyze this reaction to our knowledge. The most direct pathway is to directly decarboxylate MVA, however this pathway is not possible with our current AtPMDC. Future bioprospecting could potentially lead to a promiscuous PMDC capable of direct decarboxylation of MVA. At one extract cost of ATP, the second alternative is to decarboxylate M5P, which is closer to the canonical PMDC activity. Lastly, using the canonical pathway, we can spend 3 ATP to decarboxylate M5PP to yield isoprenol pyrophosphate (IPP), which then can be consecutively dephosphorylated to isoprenol. The second and third routes are all possible (data not shown, simple assays were set up to confirm activity). However, considering the differences in performance is very minimal, while second alternative can save one ATP usage and one reduce one enzyme usage, we chose the second alternative for future testing.

To test the ability of PMDC to produce isoprenol from mevalonic acid (MVA), the minimal systems were set up with 30 mM ATP, 2% ethanol, 50 mM MVA, 0.4 g/L PMDC. For MVA to isoprenol direct decarboxylation, no other enzymes were added. For the MVK bypass version, additional 0.1 g/L MVK and 1 g/L acid phosphatase were supplemented. For the MVK-PMVK bypass version, additional 0.1 g/L MVK, 0.2 g/L PMVK, 1 g/L NudB and 1 g/L acid phosphatase were supplemented. All reactions were let to run overnight and the isoprenol produced were extracted with 1x volume of hexane. The mixture was transferred to solvent resistant centrifuge tubes. The mixture was then vigorously vortexed and centrifuged, and the organic phase was collected for GC-FID and Gas-chromatography Mass-Spectrometry (GC-MS, Agilent 6890 Gas Chromatograph, and 5975 Inert Mass Selective Detector). The presence of isoprenol was confirmed by comparing to the retention time of standard isoprenol.
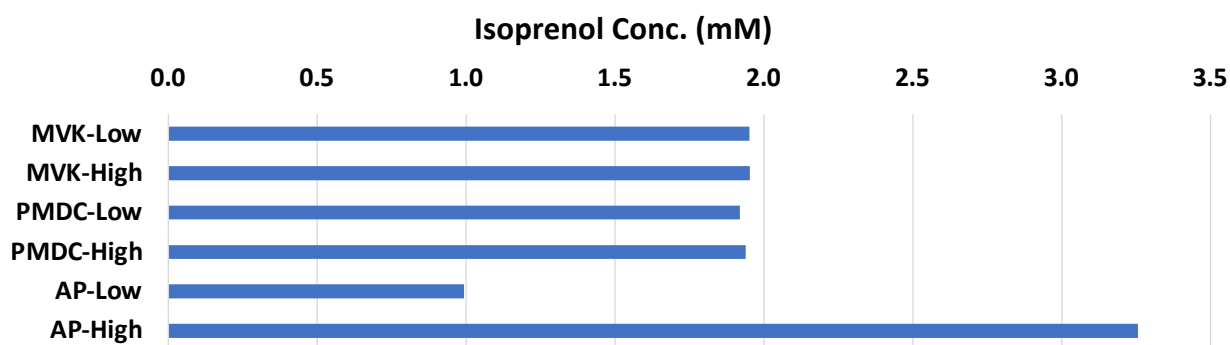
Supplemental figure 4. Bottleneck assay with either low or high enzyme loading settings) low and high setting acting as reference to which enzyme is the most bottlenecked.

With 30 mM ATP, 50 mM MVA, 2% ethanol and 0.1 g/L MVK, 0.4 g/L PMDC and 0.4 g/L AP as normal reference, MVK, PMDC and AP were either halved or doubled independent to each other one by one. The reaction mixtures were let to run overnight. And the yield was measured according to GC-FID method described in this work.
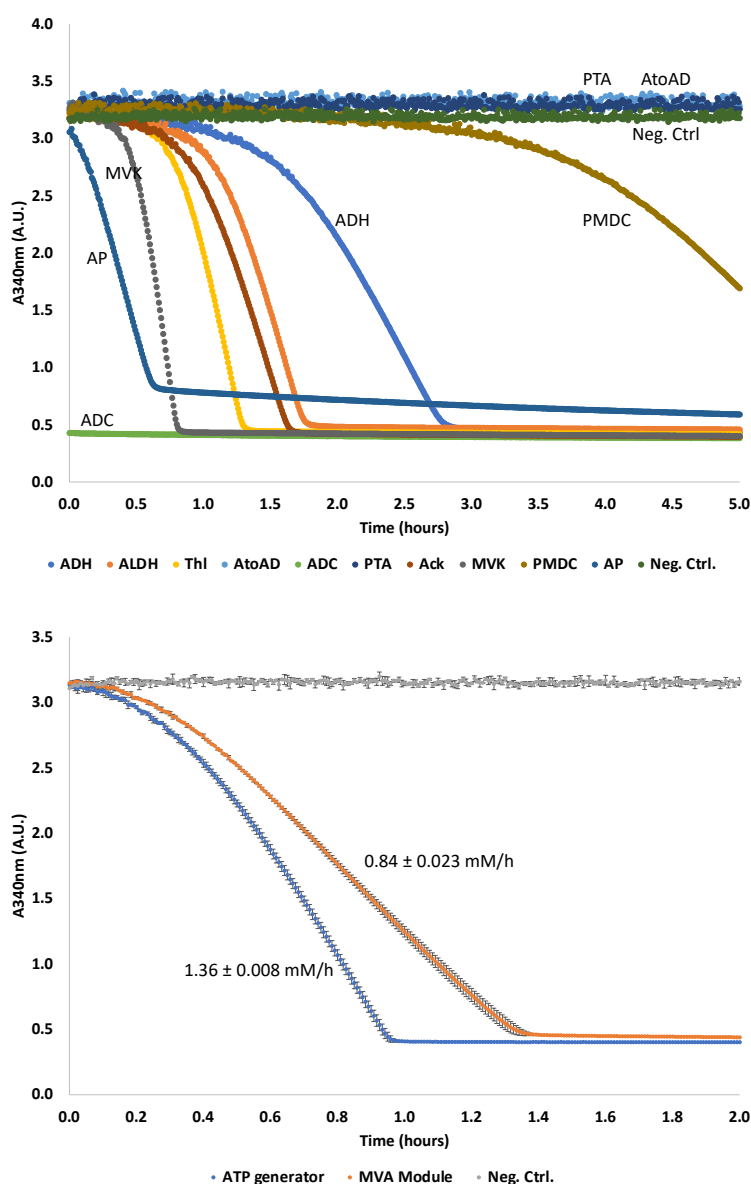
Supplemental Figure 5. ATPase contamination of all the enzymes used in the system, Upper) ATPase activities present in the enzyme samples were measured indirectly with coupled Pyruvate Kinase/Lactic Dehydrogenase (PK/LDH) assay. **Lower)** ATP generator and MVA Module pooled ATPase contamination.

To assay background ATPase activity, 5 µL of each enzyme (Nox were not shown here as its main activity is NADH oxidation which strongly interferes with PK/LDH assay) were co-incubated with PK/LDH assay mix. The method is as follows: a final concentration of master mix was made fresh with 3 mM NADH, 3 mM ATP (fresh), 3 mM Phosphoenolpyruvate, and 3 µL PK/LDH (Sigma-Aldrich P0294 from Rabbit Muscle) buffered in 195 µL General Buffer. In the presence of ATPase, ATP is hydrolyzed to ADP, which trigger the PK/LDH reaction to consume NADH. To assay enzyme samples, 5 µL of enzyme sample were mixed with 195 µL master mix. And the NADH consumptions were recorded at A340nm.

Except PTA and AtoAD, all other enzymes had varying degrees of ATPase contamination, with ADC, AP, MVK being the most contaminated. AP is notability an interesting case, where the Sigma Aldrich commercial version may not have much contamination. Hence, likely AP naturally has promiscuous activity towards ATP. Also, we were not able to isolate ATPase activity from the main activity of Nox, hence the extent of contamination of Nox enzyme sample is unknown.

All enzymes (except Nox) were pooled together according to the volume contribution in the original optimized ATP generator and MVA module set up and their ATPase contamination were assayed as previously described.

All the enzymes used in this thesis

Enzyme Symbol	Name	Source	E.C.
ADH	Alcohol Dehydrogenase	Geobacillus steaothermophilus	1.1.1.1
ALDH	Acetaldehyde Dehydrogenase	Thermus thermophilus	2.1.2.10
Nox	NADH oxidase	Lactobacillus brevis (PROSS engineered)	1.6.3.4
FDH	Formate Dehydrogenase	Burkholderia stabilis	1.17.1.9
DERA	Deoxyribose-phosphate aldolase	Thermotoga maritima	4.1.2.4
AKR	Aldo/Keto Reductase	Pseudomonas aeruginosa	1.1.1.21
Thl	Thiolase	Thermus thermophilus	2.3.1.9
PTA	Phosphate Acetyltransferase	Geobacillus steaothermophilus	2.3.1.8
ACK	Acetate Kinase	Geobacillus steaothermophilus	2.7.2.1

AtoAD	Acetate CoA-transferase	Escherichia coli	2.8.3.8
ADC	Acetoacetate Decarboxylase	Clostridium acetobutylicum	4.1.1.4
MVK	Mevalonate Kinase	methanococcus jannaschii	2.7.1.36
PMDC	Phosphomevalonate Decarboxylase	Anaerolinea thermophila	4.1.1.99
AP	Acid Phosphatase	Potato	3.1.3.2
Hex	Hexokinase	Geobacillus steaothermophilus	2.7.1.1
PMVK	Phosphomevalonate kinase	Streptococcus pyogenes	2.7.4.2
NudB	Dihydroneopterin triphosphate diphosphatase	Escherichia coli	3.6.1.67

PROSS (Protein Repair One-Stop Shop) is an online service developed by Goldenzweig, A. et al[81], which considers both the homology and the folding energy of given peptide sequence to find combinations of mutations that potentially increase the protein stability.

The DNA sequences for all enzymes used in this work

ADH

ATGAAAGCTGCAGTTGTGGAACAATTTAAAAAGCCGTTACAAGTGAAAGAAGTGGA

AAAACCTAAGATCTCATACGGGGAAGTATTAGTGCGCATCAAAGCGTGTGGGGTAT

GCCATACAGACTTGCATGCCGCACATGGCGACTGGCCTGTAAAGCCTAAACTGCCTC

TCATTCCTGGCCATGAAGGCGTCGGTGTAATTGAAGAAGTAGGTCCTGGGGTAACAC

ATTTAAAAGTTGGAGATCGCGTAGGTATCCCTTGGCTTTATTCGGCGTGCGGTCATT

GTGACTATTGCTTAAGCGGACAAGAAACATTATGCGAACGTCAACAAAACGCTGGC

TATTCCGTCGATGGTGGTTATGCTGAATATTGCCGTGCTGCAGCCGATTATGTCGTAA

AAATTCCTGATAACTTATCGTTTGAAGAAGCCGCTCCAATCTTTTGCGCTGGTGTAAC

AACATATAAAGCGCTCAAAGTAACAGGCGCAAAACCAGGTGAATGGGTAGCCATTT

ACGGTATCGGCGGGCTTGGACATGTCGCAGTCCAATACGCAAAGGCGATGGGGGTTA

AACGTCGTTGCTGTCGATTTAGGTGATGAAAAACTTGAGCTTGCTAAACAACTTGGT

GCAGATCTTGTCGTCAATCCGAAACATGATGATGCAGCACAATGGATAAAAGAAAA

AGTGGGCGGTGTGCATGCGACTGTCGTCACAGCTGTTTCAAAAGCCGCGTTCGAATC

AGCCTACAAATCCATTCGTCGCGGTGGTGCTTGCGTACTCGTCGGATTACCGCCGGA

AGAAATACCTATTCCAATTTTCGATACAGTATTAAATGGAGTAAAAATTATTGGTTC

TATCGTTGGTACGCGCAAAGACTTACAAGAGGCACTTCAATTTGCAGCAGAAGGAA

AAGTAAAAACAATTGTCGAAGTGCAACCGCTTGAAAACATTAACGACGTATTCGAT

CGTATGTTAAAAGGGCAAATTAACGGCCGCGTCGTGTTAAAAGTAGATTAA

ALDH

ATGTCCGAAAGGGGTTAAGGTAGCCATCCTGGGCTCCGGCAACATCGGGACGGACCT

GATGTACAAGCTCCTGAAGAACCCGGGCCACATGGAGCTTGTGGCGGTGGTGGGGA

TAGACCCCAAGTCCGAGGGCCTGGCCCGGGCGCGGGCCTTAGGGTTAGAGGCGAGC

CACGAAGGGATCGCCTACATCCTGGAGAGGCCGGAGATCAAGATCGTCTTTGACGC

CACCAGCGCCAAGGCCCACGTGCGCCACGCCAAGCTCCTGAGGGAGGCGGGGAAGA

TCGCCATAGACCTCACGCCGGCGGCCCGGGGCCCTTACGTGGTGCCCCCGGTGAACC

TGAAGGAACACCTGGACAAGGACAACGTGAACCTCATCACCTGCGGGGGGCAGGCC

ACCATCCCCCTGGTCTACGCGGTGCACCGGGTGGCCCCCGTGCTCTACGCGGAGATG

GTCTCCACGGTGGCCTCCCGCTCCGCGGGCCCCGGCACCCGGCAGAACATCGACGA

GTTCACCTTCACCACCGCCCGGGGCCTGGAGGCCATCGGGGGGGCCAAGAAGGGGA

AGGCCATCATCATCCTGAACCCGGCGGAACCCCCCATCCTCATGACCAACACCGTGC

GCTGCATCCCCGAGGACGAGGGCTTTGACCGGGAGGCCGTGGTGGCGAGCGTCCGG

GCCATGGAGCGGGAGGTCCAGGCCTACGTGCCCGGCTACCGCCTGAAGGCGGACCC

GGTGTTTGAGAGGCTTCCCACCCCCTGGGGGGAGCGCACCGTGGTCTCCATGCTCCT

GGAGGTGGAGGGGGCGGGGGACTATTTGCCCAAATACGCCGGCAACCTGGACATCA

TGACGGCTTCTGCCCGGAGGGTGGGGGAGGTCTTCGCCCAGCACCTCCTGGGGAAG

CCCGTGGAGGAGGTGGTGGCGTAA

Nox

ATGAAAGTTACAGTGGTTGGGTGTACGCACGCCGGCACGTTTGCAATTAAGCAAATT

CTGAAAGAGCACCCAGACGCAGAAGTCACCGTCTACGAACGTAACGATGTGATCTC

ATTTCTGTCGTGCGGAATCGCCCTGTATTTAGGAGGGCAGGTGAAGGACCCACAAGG

ATTGTTTTATTCCTCGCCAGAGGAATTACAGAAACTTGGTGCCAATGTCCAAATGAA

TCATAATGTTTTGGCCATCGATCCGGATAACAAAACAGTTACCGTCGAAGATTTGAC

GAATGGGGAGCAGTTTACTGAAAGTTATGACAAGTTGGTAATGACATCTGGATCGTG

GCCGATCGTGCCTAAAATCCCCGGTATCGACTCCGACCGCGTGCAGCTGTGTAAAAA

TTGGGCGCATGCCCAAGAGCTTTACGAGCGCGCAAAAGAGGCGAAGCGTATTGTCG

TTATTGGAGCGGGCTATATCGGTGCAGAATTGGCCGAGGCTTATAGCACAACGGGG

CATGATGTAACTCTGATTGATGCGATGGCGCGTGTCATGCCGAAATATTTCGACAAA

GAATTCACTGACGTGATCGAACAGGACTACCGCGACCATGGTGTCCAGTTAGCACTT

GGAGAGACAGTGGAATCGTTCGAGGATTCAGCCAATGGTCTGACTATTAAAACTGA

CAAGGGGTCTTATGAGACTGATTTAGCAATTCTTTGTATCGGGTTTCGCCCAAACAC

TGATTTATTAAAGGGCAAGGTGGATATGTTACCAAATGGTGCCATCATCACCGACGA

TTATATGCGCTCCTCCAACCCGGATATTTTCGCCGCTGGCGATTCTGCCGCCGTTCAT

TACAACCCTACTCATCAATATACTTACATCCCTCTTGCTACGAACGCTGTACGCCAG

GGTATCCTGGTTGGGAAAAATTTGGTTAAGCCAACCGTGAAGTACATGGGCACACA

GTCCAGCTCTGGATTAGCTCTGTACGATCGCACCATTGTAAGCACCGGCTTAACGCT

GGAGGCCGCAAAACAACTTGGCTTAAACGCCGCGCAGGTGATTGTAGAAGATAATT

ACCGTCCTGAGTTTATGCCGACCACGGAGCCGGTGTTAATGTCCCTTGTGTACGATC

CCGACACTCATCGCATCTTGGGTGGTCAGCTGATGTCTAAGTATGATGTCAGTCAGT

CCGCCAACACTTTGTCGGTTTGCATCCAGAACAAAATGACAATTGACGACCTGGCCA

TGGTCGACATGCTTTTTCAGCCCAACTTTGATCGCCCTTGGAACTACCTTAATATTCT

GGCGCAGGCTGCTCAAGCGAAGGTGGCGCAATCGGTAAACTAA

FDH

ATGGGCCTGGTGCCGCGCGGCAGCCATATGGCCACTGTATTATGCGTTCTTTATCCC

GACCCCGTTGATGGGTATCCGCCGCATTATGTCCGTGATACTATCCCCGTTATCACTC

GTTATGCTGACGGCCAAACGGCCCCGACACCTGCTGGTCCCCCGGGCTTTCGTCCTG

GGGAATTAGTGGGATCAGTCTCGGGCGCTCTTGGTCTTCGCGGCTATCTTGAGGCGC

ATGGTCACACTCTTATTGTAACGTCAGATAAAGATGGGCCGGACTCCGAATTTGAGC

GCCGCTTGCCAGATGCAGATGTTGTCATTAGCCAGCCGTTTTGGCCTGCGTATTTGAC

GGCAGAGCGTATTGCGCGCGCCCCCAAACTTCGTCTTGCGCTGACTGCAGGTATCGG

TAGCGACCACGTTGATTTAGACGCGGCGGCTCGTGCTCATATCACAGTGGCAGAGGT

TACTGGGAGCAACTCGATCTCTGTTGCCGAACACGTTGTAATGACCACGTTGGCTTT

AGTCCGTAATTATTTACCGTCACATGCGATTGCCCAACAGGGCGGCTGGAACATTGC

CGACTGTGTTTCCCGCAGCTACGATGTCGAAGGTATGCATTTTGGTACAGTTGGGGC

TGGGCGCATCGGATTGGCGGTACTGCGTCGCCTTAAGCCATTTGGTCTGCACTTACA

CTATACCCAACGTCACCGTTTGGACGCCGCCATCGAACAAGAATTAGGTCTGACCTA

TCACGCTGATCCCGCGTCGCTTGCAGCAGCTGTAGATATCGTTAATTTGCAAATTCC

ACTTTACCCCTCAACTGAGCACCTTTTTGACGCGGCGATGATTGCCCGTATGAAGCG

CGGAGCCTACTTAATTAATACGGCGCGCGCTAAATTAGTCGATCGTGATGCAGTAGT

TCGTGCGGTTACGTCAGGCCATCTTGCTGGTTATGGGGGTGACGTATGGTTTCCGCA

GCCCGCACCGGCAGACCATCCGTGGCGTGCTATGCCGTTCAATGGGATGACACCTCA

TATTTCAGGAACAAGTCTTTCTGCTCAAGCACGTTACGCGGCTGGTACCCTTGAGAT

CTTGCAGTGCTGGTTCGACGGTCGCCCTATTCGTAATGAGTACCTGATCGTAGATGG

AGGTACACTTGCGGGTACGGGGGCGCAGAGCTATCGTCTTACCTAA

DERA

ATGATCGAGTACCGCATTGAGGAAGCCGTCGCCAAGTATCGTGAGTTTTATGAGTTT

AAGCCTGTGCGCGAGAGCGCCGGCATTGAGGACGTTAAGTCAGCAATTGAGCATAC

CAACCTCAAGCCATTTGCCACACCTGATGATATCAAGAAGTTATGTCTGGAAGCGCG

TGAAAATCGCTTTCACGGCGTGTGCGTTAATCCATGTTATGTTAAGCTTGCGCGCGA

AGAATTAGAGGGCACCGACGTGAAGGTCGTCACAGTGGTTGGCTTCCCCCTCGGGG

CGAACGAGACCCGCACTAAGGCACACGAGGCTATCTTCGCGGTAGAAAGTGGCGCC

GACGAGATTGACATGGTCATCAATGTTGGCATGCTGAAAGCGAAGGAATGGGAATA

CGTGTATGAGGATATCCGTTCGGTGGTGGAGAGCGTCAAGGGTAAGGTGGTAAAAG

TGATTATCGAGACCTGTTATTTAGATACTGAGGAGAAGATCGCGGCATGCGTGATCA

GCAAGCTGGCGGGCGCTCATTTCGTGAAGACTTCGACGGGATTTGGTACCGGTGGTG

CGACAGCGGAAGACGTGCATTTGATGAAGTGGATCGTGGGAGATGAGATGGGTGTG

AAGGCGTCCGGTGGTATTCGTACCTTCGAAGATGCTGTCAAGATGATTATGTATGGC

GCAGACCGCATTGGCACATCAAGTGGCGTAAAGATTGTACAAGGCGGTGAGGAGCG

TTACGGTGGTTGA

AKR

ATGTCAGTGGAAAGCATCCGCATTGAAGGCATCGACACCCCAGTTAGTCGTATTGGG

TTGGGTACCTGGGCGATTGGTGGATGGATGTGGGGCGGCGCGGACGACGCGACCAG

CGTTGAGACGATCCGTCGTGCTGTGGAAAGTGGTATTAATCTCATCGATACAGCACC

CGTGTATGGATTCGGCCACTCAGAAGAGGTCGTCGGAAAGGCCCTGCAAGGTTTGC

70

GCGATAAGGCGGTGATTGCAACGAAAGCAGCGCTTGAGTGGAGCGATGCAGGTATT

CACCGCAATGCTTCGGCCGCCCGTATCCGTCGCGAGGTTGAGGACTCTCTGCGCCGC

TTGAAGACTGATCGTATCGACCTCTACCAGATTCATTGGCCGGACCCTCTTGTGGCTC

ATGAAGAGACAGCTGGTGAGCTCGAGCGCCTGCGTCGCGACGGCAAGATTCTCGCA

ATTGGCGTGAGCAATTATTCACCAGAGCAGATGGACGGGTTCCGCCAATTTGCACCA

TTGGCATCGGTCCAACCACCCTACAATCTTTTCGAGCGTGCAATCGACGCGGACGTC

CTTCCCTATGCAGAACGCAACGGTATCGTTGTATTGGCATATGGCGCGCTTTGCCGC

GGTTTGTTATCTGGCCGCATGAATGCGGAGACCCGCTTCGACGGTGATGACCTGCGT

AAGAGCGACCCAAAATTTCAACAACCTCGCTTCGCGCAATATCTGGCGGCAGTAGC

GCAGTTAGAGGAGTTAGCACGTGAGCGTTATGGAAAGAGTGTATTAGCTCTCGCAAT

CCGCTGGATTCTCGATCGTGGCCCGACAGTGGCACTGTGGGGAGCGCGCAAACCAG

AGCAATTAAATGGAATCGCGGACGCATTTGGGTGGCGTCTCGACGACGAGGCAATG

GCGCGCATCGAACGCATCTTAGCGGAGACCATTCAGGACCCGGTAGGCCCCGAGTTT

ATGGCGCCGCCAAGTCGTAATGCGTGA

Thl

ATGCGTGAAGTGTATGTAGTCGCGGCAGTCCGTACCCCAATCGGCAAATTTGGCGGC

GTATTCAAGGACGTTAGTCCCGTTGACTTAGGCGCGCACGCGATGCGTGAAGCATTA

GCTCGTGCGGGGGTAGAGGGAAAGGCGTTGGATTTGTATATCTTCGGAAATGTTCTT

CGCGCAGGACACGGCCAATTGTTACCGCGCCAAGCGGCGTTGAAGGCCGGTATCCC

CAAAGAGGTCGACGGGTACCAAGTCGACATGGTGTGTGCCAGTGGCATGATGGCCG

CGCTGAACGCGGTTCAATTCTTACGTACCGGCGAGGCCCATCTTGTGCTGGCCGGTG

GGATGGAGTCAATGTCCCAAGCGGGTTTTTATCTTAGCCACCGTGCCCGTTGGGGGT

ATAAATTTTTACTTGGTGCACCCGAAAATCTTCAGGATATCCTGCTTCGTGATGGACT

GTCGGACCCATTTACCGGCGAAGCGATGGGTGAGCAGGCCGAACGCTTAGCTCAGG

ATCATGGTGTGACTCGCCGCGAAATTGATGAAGCGGCCTATCTGAGTCACAAGCGCG

CTGCGGAGGCCACTGAAAAGGGCCTTTTCGCGTGGGAGATTGCGCCGATGGAGGTG

CAGGGTCGTAAAGGCCCCGTAGTCGTGGACCGCGACGAGGGAATCCGTCCTGAAAC

TACACTTGAGAGCTTGGCGGCTTTGCGCCCGGCGTTCAAAAAAGATGGAGTGCTGAC

CGCAGGAAATTCATCTCAGATCTCGGACGGCGCAGCGGCTTTGCTTCTTGCGTCAGA

AGAAGCTGTGAAAGCCCACGGGCTTAAGCCAATTGCGAAGGTACTGGGGGGCGCGT

GGGCTGCTGGGGAGTCATGGCGTTTCCCTGAAGCACCGATTCCGGCTGCTAAACGCT

TACTGGACCGTTTAGGCATGCGCGTGTCTGATTTCGGGCTTTTCGAGAATAACGAAG

CGTTCGCATTGAATAATGTCCTGTTTTCCCGTCTGCTGGATGTTCCCTACGAGCGCTT

GAATGTGTTCGGTGGCGCTGTAGCCTTGGGACATCCTATTGGAGCGAGTGGAGCACG

CATTTTGGTGACCTTACTGAATGCGTTACGTGCGAAGGGCGAGGAGCGCGGGCTTGC

CGCAATCTGTCATGGTACAGGTGGTAGTGTTGCTTTCGCGGTTGAAGTAGTATAA

PTA

ATGACAACCGATTTATTTACGGCATTAAAAGCGAAAGTAACCGGTACGGCTCGAAA

AATCGTGTTTCCCGAGGGAACCGATGACCGCATCTTAACGGCGGCGAGCCGTTTGGC

GACGGAGCAAGTGCTTCAGCCGATCGTCCTTGGCGATGAGCAAGCGATAAGGGTGA

AAGCAGCTGCGCTTGGCTTGCCGCTTGAAGGGGTGGAGATTGTCAACCCGCGCCGCT

ACGGCGGGTTTGATGAGCTAGTTTCGGCGTTTGTGGAGCGGCGCAAAGGGAAAGTG

72

ACAGAAGAAACGGCGCGCGAGTTGCTTTTCGATGAAAACTATTTCGGTACGATGCTC

GTTTATATGGGAGCGGCCGACGGCCTCGTCAGCGGGGCGGCACATTCGACGGCGGA

TACGGTCCGACCAGCCTTGCAAATCATTAAAACGAAGCCAGGCGTTGACAAAACGT

CCGGCGTGTTCATCATGGTGCGCGGCGACGAAAAATATGTGTTTGCCGATTGCGCCA

TCAACATTGCTCCTAACAGTCATGATTTGGCTGAAATCGCGGTCGAGAGCGCCCGGA

CGGCCAAAATGTTCGGCCTTAAGCCGCGCGTAGTGCTGTTAAGCTTTTCCACGAAAG

GGTCGGCCTCGTCGCCGGAGACGGAAAAAGTCGTTGAGGCGGTGCGGTTGGCGAAA

GAAATGGCGCCGGATCTGATCCTTGACGGTGAGTTTCAATTTGACGCCGCGTTTGTG

CCAGAGGTGGCGAAAAAGAAAGCGCCGGACTCGGTCATTCAAGGGGACGCAAATGT

CTTTATTTTCCCGAGCCTTGAGGCGGGCAACATCGGCTACAAAATCGCCCAGCGCCT

TGGCGGCTTTGAAGCGGTTGGCCCGATTTTGCAAGGGCTGAACAAGCCGGTTAACGA

CCTATCGCGCGGCTGCAGCGCCGAAGACGCCTACAAGCTCGCGCTCATCACCGCGGC

GCAGTCGCTTGGGGAGTAA

ACK

ATGGCAAAAGTGTTAGCCGTTAATGCGGGAAGTTCTTCGTTGAAATTCCAATTGTTT

GACATGCCGGCGGAAACGGTGTTAACGAAAGGAATCGTCGAGCGGATCGGCTTTGA

CGACGCGATTTTTACGATCGTCGTGAACGGGGAGAAACAGCGGGAAGTCACTTCCA

TCCCGAACCATGCCGTGGCGGTGAAACTGCTGCTTGACAAACTGATTCGCTATGGCA

TCATCCGGTCATTTGACGAAATTGACGGCATCGGCCATCGCGTCGTCCACGGCGGGG

AGAAGTTCAGCGATTCGGTGTTGATCACCGATGAGGTGATAAAACAAATCGAAGAA

GTGTCCGAGCTCGCTCCGCTTCATAACCCGGCCAACCTCGTCGGCATCCGCGCGTTT

CAGGAAGTGCTGCCGAACGTGCCGGCCGTCGCCGTTTTTGATACGGCGTTTCACCAA

ACGATGCCGGAACAGTCGTTTTTGTACAGCTTGCCGTATGAGTATTACACGAAATTC

GGCATTCGCAAGTACGGCTTCCATGGCACGTCGCACAAATACGTCACCCAGCGGGC

GGCGGAGCTTCTCGGCCGGCCGATCGAGCAGCTGCGCCTCATCTCGTGCCATTTAGG

CAACGGGGCGAGCATCGCGGCGGTCGAAGGCGGCAAATCGATCGACACGTCGATGG

GCTTTACGCCATTAGCGGGCGTCGCGATGGGGACGCGCTCTGGCAACATCGACCCGG

CGCTTATCCCATACATTATGGAAAAACAGGAATGACCGTTAATGAAGTGATTGAA

GTGCTGAATAAAAAGAGCGGCATGCTCGGCATCTCCGGCATCTCGAGCGACTTGCGC

GACTTGGAAAAAGCGGCCGCCGAAGGAAATGAGCGCGCGGAACTTGCGTTGGAAGT

GTTTGCGAACCGCATTCATAAATACATCGGCTCGTATGCGGCGCGCATGTGCGGCGT

CGACGCCATCATTTTCACCGCCGGCATCGGCGAAAACAGCGAAGTCGTGCGGGCCA

AAGTGTTGCGCGGCCTCGAGTTTATGGGAGTTTACTGGGATCCCATCCTAAACAAAG

TGCGCGGCAAAGAAGCGTTCATCAGCTACCCGCACTCGCCGGTCAAAGTGCTCGTCA

TCCCGACGAACGAAGAGGTCATGATCGCCCGTGATGTCATGCGGCTGGCGAATTTGT

AA

AtoAD complex

ATGAAAACAAAATTGATGACATTACAAGACGCCACCGGCTTCTTTCGTGACGGCATG

ACCATCATGGTGGGCGGATTTATGGGGATTGGCACTCCATCCCGCCTGGTTGAAGCA

TTACTGGAATCTGGTGTTCGCGACCTGACATTGATAGCCAATGATACCGCGTTTGTT

GATACCGGCATCGGTCCGCTCATCGTCAATGGTCGAGTCCGCAAAGTGATTGCTTCA

CATATCGGCACCAACCCGGAAACAGGTCGGCGCATGATATCTGGTGAGATGGACGT

74

CGTTCTGGTGCCGCAAGGTACGCTAATCGAGCAAATTCGCTGTGGTGGAGCTGGACT

TGGTGGTTTTCTCACCCCAACGGGTGTCGGCACCGTCGTAGAGGAAGGCAAACAGA

CACTGACACTCGACGGTAAAACCTGGCTGCTCGAACGCCCACTGCGCGCCGACCTGG

CGCTAATTCGCGCTCATCGTTGCGACACACTTGGCAACCTGACCTATCAACTTAGCG

CCCGCAACTTTAACCCCCTGATAGCCCTTGCGGCTGATATCACGCTGGTAGAGCCAG

ATGAACTGGTCGAAACCGGCGAGCTGCAACCTGACCATATTGTCACCCCTGGTGCCG

TTATCGACCACATCATCGTTTCACAGGAGAGCAAATAA*TGGATGCGAAACAACGTATT*

GCGCGCCGTGTGGCGCAAGAGCTTCGTGATGGTGACATCGTTAACTTAGGGATCGGTTTA

*CCCACA*ATGGTCGCCAATTATTTACCGGAGGGTATTCATATCACTCTGCAATCGGAA

AACGGCTTCCTCGGTTTAGGCCCGGTCACGACAGCGCATCCAGATCTGGTGAACGCT

GGCGGGCAACCGTGCGGTGTTTTACCCGGTGCAGCCATGTTTGATAGCGCCATGTCA

TTTGCGCTAATCCGTGGCGGTCATATTGATGCCTGCGTGCTCGGCGGTTTGCAAGTA

GACGAAGAAGCAAACCTCGCGAACTGGGTAGTGCCTGGGAAAATGGTGCCCGGTAT

GGGTGGCGCGATGGATCTGGTGACCGGGTCGCGCAAAGTGATCATCGCCATGGAAC

ATTGCGCCAAAGATGGTTCAGCAAAAATTTTGCGCCGCTGCACCATGCCACTCACTG

CGCAACATGCGGTGCATATGCTGGTTACTGAACTGGCTGTCTTTCGTTTTATTGACGG

CAAAATGTGGCTCACCGAAATTGCCGACGGGTGTGATTTAGCCACCGTGCGTGCCAA

AACAGAAGCTCGGTTTGAAGTCGCCGCCGATCTGAATACGCAACGGGGTGATTTATG

A (italic blue region is the linker sequence)

ADC

ATGCTCAAAGATGAAGTTATTAAGCAGATCAGTACCCCGTTAACCTCTCCGGCATTC

CCACGTGGCCCTTACAAATTCCATAACCGTGAATACTTTAACATCGTTTATCGTACTG

ATATGGACGCCCTGCGCAAAGTTGTGCCCGAACCCCTCGAGATCGATGAACCGCTCG

TGCGCTTTGAAATTATGGCAATGCATGATACCTCAGGGCTGGGATGTTATACGGAGT

CTGGTCAGGCCATTCCGGTCAGCTTCAATGGGGTAAAAGGGGATTACCTCCATATGA

TGTACCTCGATAATGAACCGGCAATTGCGGTGGGCCGCGAACTGAGCGCATATCCG

AAAAAACTGGGGTATCCGAAACTGTTCGTTGACAGCGATACGTTGGTTGGCACCCTC

GATTATGGAAAACTGCGCGTGGCGACTGCTACCATGGGGTACAAGCACAAAGCCTT

GGACGCGAACGAGGCGAAGGACCAAATTTGCCGTCCTAACTATATGCTTAAGATTAT

TCCCAATTATGATGGATCTCCGCGTATTTGCGAACTCATTAATGCCAAAATTACCGA

CGTTACGGTTCATGAGGCATGGACAGGCCCGACCCGCTTGCAACTGTTTGACCACGC

CATGGCCCCGCTGAATGATTTACCGGTAAAAGAAATTGTATCCAGTAGCCATATCTT

GGCCGATATTATCTTGCCGCGCGCGGAAGTTATTTACGATTATCTGAAATAA

MVK

ATGATTATTGAAACCCCATCCAAAGTTATCTTATTCGGGGAGCACGCAGTAGTATAT

GGGTACCGCGCAATTTCAATGGCTATTGATTTAACGTCAACGATCGAGATTAAGGAG

ACGCAGGAAGACGAAATCATCCTTAATCTGAACGACCTGAACAAAGTCTGGGCTT

GAATTTGAACGAGATCAAGAATATCAATCCAAACAATTTCGGGGACTTTAAGTACTG

TCTGTGCGCTATTAAAAATACCTTAGATTACCTTAATATCGAGCCTAAGACCGGCTT

CAAAATTAACATCTCTTCGAAGATTCCCATCTCGTGCGGGCTTGGTTCCAGTGCGTC

GATTACCATCGGAACTATCAAAGCTGTCAGCGGCTTTTACAACAAAGAATTGAAAG

ATGATGAAATTGCAAAATTAGGCTACATGGTAGAAAAGGAGATCCAAGGGAAAGCT

AGTATCACCGACACGAGCACCATCACTTACAAGGGGATTTTGGAGATTAAGAACAA

TAAGTTTCGCAAAATTAAAGGCGAATTTGAAGAGTTCCTGAAGAACTGCAAATTCTT

AATCGTTTACGCAGAGAAGCGTAAGAAGAAGACCGCCGAGCTTGTAAATGAGGTTG

CGAAAATTGAAAATAAGGACGAGATCTTCAAAGAGATTGATAAGGTCATTGACGAG

GCTCTGAAGATTAAAAACAAGGAAGACTTCGGAAAACTTATGACAAAAAATCATGA

GTTACTTAAAAAGTTGAACATCAGTACCCCAAAGCTGGACCGCATCGTAGATATTGG

AAACCGTTTTGGATTCGGGGCGAAATTAACCGGAGCGGGAGGAGGTGGTTGCGTCA

TTATTTTAGTTAATGAAGAGAAGGAGAAGGAGCTGCTTAAGGAGCTGAATAAGGAG

GATGTTCGTATTTTCAACTGCCNTATGANGAATTAA

PMDC

ATGGGCCAGGCGACCGCCATCGCGCATCCGAACATTGCTTTCATTAAATATTGGGGT

AATCGCGACGCCGTTCTTCGTATTCCGGAAAATGGCAGTATTTCAATGAATCTGGCC

GAACTGACTGTAAAAACCACGGTTATTTTTGAAAAACATTCTCGTGAAGATACGCTG

ATCTTAAACGGCGCTCTGGCGGATGAACCGGCGCTGAAACGCGTTTCGCACTTTCTT

GATCGCGTACGCGAGTTTGCAGGCATTTCGTGGCACGCACATGTTATTAGCGAGAAC

AACTTTCCGACTGGGGCCGGTATCGCGTCAAGCGCCGCCGCCTTTGCCGCGCTCGCG

CTGGCCGCGACCTCTGCTATTGGTCTGCATTTAAGTGAACGTGATCTGAGCCGCCTC

GCCCGCAAAGGGTCCGGCTCGGCGTGTCGCTCAATTCCTGGCGGTTTCGTCGAGTGG

ATCCCGGGCGAGACGGATGAAGATTCCTATGCAGTGTCGATCGCCCCGCCCGAACAT

TGGGCCCTGACCGATTGCATTGCGATTTTGAGTACCCAGCATAAACCCATCGGTTCT

ACTCAGGGTCATGCACTGGCCAGTACATCCCCCCTGCAGCCGGCGCGCGTGGCGGAT

ACTCCTCGTCGGCTGGAAATTGTCCGTCGTGCGATTCTCGAACGTGATTTTCTGTCGC

TCGCCGAAATGATCGAACATGATTCCAACCTGATGCACGCAGTTATGATGACGTCAA

CCCCGCCCTTATTTTATTGGGAACCGGTGAGCCTTGTAATCATGAAATCTGTGCGCG

AATGGCGCGAATCTGGTCTCCCTTGCGCCTACACTTTGGATGCCGGTCCGAACGTGC

ACGTGATTTGCCCCTCCGAATATGCAGAGGAAGTGATTTTTCGGCTGACGAGCATTC

CAGGTGTGCAAACGGTCCTTAAGGCCTCTGCTGGTGATTCAGCCAAGCTGATCGAGC

AGTCCCTGTAA

Hex

ATGCCAAAATTAAAATTAATCGGTGTTGACTTAGGTGGAACTACTTTCAGCGTTGGG

CTTGTTAGCGAAGATGGTAAAATTCTGAAGAAAGTTACGCGCGACACGTTGGTCGA

AAACGGAAAGGAGGATGTTATTCGTCGTATTGCAGAAACGATCTTAGAAGTATCCG

ATGGAGAGGAGGCGCCTTACGTGGGAATTGGGAGTCCGGGCAGCATCGACCGCGAA

AACGGCATCGTTCGTTTCAGCCCAAATTTCCCTGATTGGCATAATGTGCCCCTGACTG

ACGAACTGGCTAAGCGTACAGGGAAAAAGGTATTTCTGGAAAACGATGCTAATGCC

TTTGTGCTTGGGGAAAAATGGTTTGGAGCCGGACGTGGTCACGATCACATCGTTGCG

CTGACGCTTGGGACAGGGATCGGAGGTGGGGTTGTAACTCACGGATACTTGTTGACG

GGGCGTGACGGGATTGGTGCAGAGTTGGGACACGTCGTGGTGGAGCCTAATGGACC

TATGTGTAACTGTGGGACGCGCGGATGTCTGGAGGCTGTCGCTTCAGCCACTGCAAT

CCGCCGCTTTCTGCGCGAGGGATATAAAAAGTACCATTCTTCATTAGTCTATAAGCT

TGCAGGTAGCCCCGAGAAGGCTGACGCGAAGCACTTGTTTGACGCGGCGCGTCAAG

GGGATCGTTTTGCGCTGATGATCCGTGACCGCGTTGTTGACGCTTTGGCTCGCGCCGT

TGCAGGTTATATTCATATCTTTAACCCCGAAATCGTTATTATTGGAGGTGGCATTTCA

CGTGCTGGAGAGATTTTGTTCGGTCCCCTTCGCGAAAAGGTCGTTGACTATATTATG

CCCAGTTTCGTAGGGACGTATGAGGTGGTGGCCTCACCATTGGTAGAGGACGCGGGT

ATTTTGGGAGCGGCCTCGATCATTAAGGAGCGTATTGGCGCGTAA

References

1. World Population Prospects - Population Division - United Nations. https://population.un.org/wpp/Graphs/Probabilistic/POP/TOT/900.

2. Tripathy, D. B. Applications of Petrochemicals: A Mini Review. *Recent Adv. Petrochem. Sci.* **2**, (2017).

3. Kätelhön, A., Meys, R., Deutz, S., Suh, S. & Bardow, A. Climate change mitigation potential of carbon capture and utilization in the chemical industry. *Proc. Natl. Acad. Sci.* **116**, 11187–11194 (2019).

4. Birol, D. F. Tracking Clean Energy Progress 2017. 116.

5. Albers, S. C., Berklund, A. M. & Graff, G. D. The rise and fall of innovation in biofuels. *Nat. Biotechnol.* **34**, 814–821 (2016).

6. Advanced Algal Systems. *Energy.gov* https://www.energy.gov/eere/bioenergy/advanced-algal-systems.

7. Adeniyi, O. M., Azimov, U. & Burluka, A. Algae biofuel: Current status and future applications. *Renew. Sustain. Energy Rev.* **90**, 316–335 (2018).

8. Keasling, J. *et al.* Microbial production of advanced biofuels. *Nat. Rev. Microbiol.* **19**, 701–715 (2021).

9. Jouny, M., Luc, W. & Jiao, F. General Techno-Economic Analysis of CO2 Electrolysis Systems. *Ind. Eng. Chem. Res.* **57**, 2165–2177 (2018).

10. Alternative Fuels Data Center: Ethanol Fuel Basics. https://afdc.energy.gov/fuels/ethanol_fuel_basics.html.

11. Amorim, H. V., Lopes, M. L., de Castro Oliveira, J. V., Buckeridge, M. S. & Goldman, G. H. Scientific challenges of bioethanol production in Brazil. *Appl. Microbiol. Biotechnol.* **91**, 1267–1275 (2011).

12. Sanz-Pérez, E. S., Murdock, C. R., Didas, S. A. & Jones, C. W. Direct Capture of CO_2 from Ambient Air. *Chem. Rev.* **116**, 11840–11876 (2016).

13. Use of ethanol - U.S. Energy Information Administration (EIA). https://www.eia.gov/energyexplained/biofuels/use-and-supply-of-ethanol.php.

14. Robak, K. & Balcerek, M. Review of Second Generation Bioethanol Production from Residual Biomass. *Food Technol. Biotechnol.* **56**, 174–187 (2018).

15. LanzaTech | Capturing carbon. Fueling growth. https://www.lanzatech.com/.

16. Debut Biotech. *Debut Biotech* https://debutbiotech.com/.

17. Invizyne. *Invizyne* https://www.invizyne.com.

18. Zhang, W. *et al.* Progress and Perspective of Electrocatalytic CO2 Reduction for Renewable Carbonaceous Fuels and Chemicals. *Adv. Sci.* **5**, 1700275 (2018).

19. Fairley, P. Energy storage: Power revolution. *Nature* **526**, S102–S104 (2015).

20. Yishai, O., Goldbach, L., Tenenboim, H., Lindner, S. N. & Bar-Even, A. Engineered Assimilation of Exogenous and Endogenous Formate in *Escherichia coli*. *ACS Synth. Biol.* **6**, 1722–1731 (2017).

21. Bowie, J. U. *et al.* Synthetic Biochemistry: The Bio-inspired Cell-Free Approach to Commodity Chemical Production. *Trends Biotechnol.* **38**, 766–778 (2020).

22. Cai, T. *et al.* Cell-free chemoenzymatic starch synthesis from carbon dioxide. *Science* **373**, 1523–1527 (2021).

23. Series A - Debut Biotech - 2021-08-12 - Crunchbase Funding Round Profile. *Crunchbase* https://www.crunchbase.com/funding_round/debut-biotech-series-a--205dfc9f.

24. You, C. *et al.* An in vitro synthetic biology platform for the industrial biomanufacturing of myo-inositol from starch. *Biotechnol. Bioeng.* **114**, 1855–1864 (2017).

25. Sherkhanov, S. *et al.* Isobutanol production freed from biological limits using synthetic biochemistry. *Nat. Commun.* **11**, 4292 (2020).

26. Hoekman, S. K. & Broch, A. Environmental implications of higher ethanol production and use in the U.S.: A literature review. Part II – Biodiversity, land use change, GHG emissions, and sustainability. *Renew. Sustain. Energy Rev.* **81**, 3159–3177 (2018).

27. De Tissera, S. *et al.* Syngas Biorefinery and Syngas Utilization. *Adv. Biochem. Eng. Biotechnol.* **166**, 247–280 (2019).

28. Müller, V. New Horizons in Acetogenic Conversion of One-Carbon Substrates and Biological Hydrogen Storage. *Trends Biotechnol.* **37**, 1344–1354 (2019).

29. Handler, R. M., Shonnard, D. R., Griffing, E. M., Lai, A. & Palou-Rivera, I. Life Cycle Assessments of Ethanol Production via Gas Fermentation: Anticipated Greenhouse Gas Emissions for Cellulosic and Waste Gas Feedstocks. *Ind. Eng. Chem. Res.* **55**, 3253–3261 (2016).

30. Verma, S., Kim, B., Jhong, H.-R. "Molly", Ma, S. & Kenis, P. J. A. A Gross-Margin Model for Defining Technoeconomic Benchmarks in the Electroreduction of CO2. *ChemSusChem* **9**, 1972–1979 (2016).

31. Wang, X. *et al.* Efficient electrically powered CO 2 -to-ethanol via suppression of deoxygenation. *Nat. Energy* **5**, 478–486 (2020).

32. Kwok, R. Five hard truths for synthetic biology. *Nature* **463**, 288–290 (2010).

33. Stephanopoulos, G. Challenges in Engineering Microbes for Biofuels Production. *Science* **315**, 801–804 (2007).

34. Chubukov, V., Mukhopadhyay, A., Petzold, C. J., Keasling, J. D. & Martín, H. G. Synthetic and systems biology for microbial production of commodity chemicals. *Npj Syst. Biol. Appl.* **2**, 1–11 (2016).

35. Lin, P. P. *et al.* Construction and evolution of an Escherichia coli strain relying on nonoxidative glycolysis for sugar catabolism. *Proc. Natl. Acad. Sci. U. S. A.* **115**, 3538–3546 (2018).

36. Bogorad, I. W., Lin, T.-S. & Liao, J. C. Synthetic non-oxidative glycolysis enables complete carbon conservation. *Nature* **502**, 693–697 (2013).

37. Zhang, L. *et al.* An artificial synthetic pathway for acetoin, 2,3-butanediol, and 2-butanol production from ethanol using cell free multi-enzyme catalysis. *Green Chem.* **20**, 230–242 (2018).

38. Opgenorth, P. H., Korman, T. P. & Bowie, J. U. A synthetic biochemistry molecular purge valve module that maintains redox balance. *Nat. Commun.* **5**, 4113 (2014).

39. Flamholz, A., Noor, E., Bar-Even, A. & Milo, R. eQuilibrator—the biochemical thermodynamics calculator. *Nucleic Acids Res.* **40**, D770–D775 (2012).

40. Nemr, K. *et al.* Engineering a short, aldolase-based pathway for (R)-1,3-butanediol production in Escherichia coli. *Metab. Eng.* **48**, 13–24 (2018).

41. Kim, T. *et al.* Rational engineering of 2-deoxyribose-5-phosphate aldolases for the biosynthesis of (R)-1,3-butanediol. *J. Biol. Chem.* **295**, 597–609 (2020).

42. Kim, T. *et al.* Novel Aldo-Keto Reductases for the Biocatalytic Conversion of 3-Hydroxybutanal to 1,3-Butanediol: Structural and Biochemical Studies. *Appl. Environ. Microbiol.* **83**, (2017).

43. Haridas, M., Abdelraheem, E. M. M. & Hanefeld, U. 2-Deoxy-d-ribose-5-phosphate aldolase (DERA): applications and modifications. *Appl. Microbiol. Biotechnol.* **102**, 9959–9971 (2018).

44. Sakuraba, H. *et al.* Sequential Aldol Condensation Catalyzed by Hyperthermophilic 2-Deoxy-d-Ribose-5-Phosphate Aldolase. *Appl. Environ. Microbiol.* **73**, 7427–7434 (2007).

45. Carbon neutrality by 2050: the world's most urgent mission | United Nations Secretary-General. https://www.un.org/sg/en/content/sg/articles/2020-12-11/carbon-neutrality-2050-the-world%E2%80%99s-most-urgent-mission.

46. Kätelhön, A., Meys, R., Deutz, S., Suh, S. & Bardow, A. Climate change mitigation potential of carbon capture and utilization in the chemical industry. *Proc. Natl. Acad. Sci.* **116**, 11187–11194 (2019).

47. Sakai, S. *et al.* Acetate and ethanol production from H2 and CO2 by Moorella sp. using a repeated batch culture. *J. Biosci. Bioeng.* **99**, 252–258 (2005).

48. Handler, R. M., Shonnard, D. R., Griffing, E. M., Lai, A. & Palou-Rivera, I. Life Cycle Assessments of Ethanol Production via Gas Fermentation: Anticipated Greenhouse Gas Emissions for Cellulosic and Waste Gas Feedstocks. *Ind. Eng. Chem. Res.* **55**, 3253–3261 (2016).

49. Köpke, M., Mihalcea, C., Bromley, J. C. & Simpson, S. D. Fermentative production of ethanol from carbon monoxide. *Curr. Opin. Biotechnol.* **22**, 320–325 (2011).

50. De Tissera, S. *et al.* Syngas Biorefinery and Syngas Utilization. *Adv. Biochem. Eng. Biotechnol.* **166**, 247–280 (2019).

51. Handoko, A. D., Chan, K. W. & Yeo, B. S. –CH3 Mediated Pathway for the Electroreduction of CO2 to Ethane and Ethanol on Thick Oxide-Derived Copper Catalysts at Low Overpotentials. *ACS Energy Lett.* **2**, 2103–2109 (2017).

52. Xu, H. *et al.* Highly selective electrocatalytic CO2 reduction to ethanol by metallic clusters dynamically formed from atomically dispersed copper. *Nat. Energy* **5**, 623–632 (2020).

53. Cheng, Y., Hou, J. & Kang, P. Integrated Capture and Electroreduction of Flue Gas CO2 to Formate Using Amine Functionalized SnOx Nanoparticles. *ACS Energy Lett.* **6**, 3352–3358 (2021).

54. Wang, X. *et al.* Efficient electrically powered CO 2 -to-ethanol via suppression of deoxygenation. *Nat. Energy* **5**, 478–486 (2020).

55. Dagle, R. A., Winkelman, A. D., Ramasamy, K. K., Lebarbier Dagle, V. & Weber, R. S. Ethanol as a Renewable Building Block for Fuels and Chemicals. *Ind. Eng. Chem. Res.* **59**, 4843–4853 (2020).

56. Liu, H. & Bowie, J. U. Cell-free synthetic biochemistry upgrading of ethanol to 1,3 butanediol. *Sci. Rep.* **11**, 9449 (2021).

57. Flamholz, A., Noor, E., Bar-Even, A. & Milo, R. eQuilibrator—the biochemical thermodynamics calculator. *Nucleic Acids Res.* **40**, D770–D775 (2012).

58. Temperature affects dissolved oxygen concentrations | U.S. Geological Survey. https://www.usgs.gov/media/images/temperature-affects-dissolved-oxygen-concentrations.

59. Chen, H. & Zhang, Y.-H. P. J. Enzymatic regeneration and conservation of ATP: challenges and opportunities. *Crit. Rev. Biotechnol.* **41**, 16–33 (2021).

60. Suryatin Alim, G., Iwatani, T., Okano, K., Kitani, S. & Honda, K. In Vitro Production of Coenzyme A Using Thermophilic Enzymes. *Appl. Environ. Microbiol.* **87**, e0054121 (2021).

61. Li, M. *et al.* Recent advances of metabolic engineering strategies in natural isoprenoid production using cell factories. *Nat. Prod. Rep.* **37**, 80–99 (2020).

62. Ninnemann, E. *et al.* Co-optima fuels combustion: A comprehensive experimental investigation of prenol isomers. *Fuel* **254**, 115630 (2019).

63. Dugar, D. & Neltner, B. Processes for conversion of biologically derived mevalonic acid. (2016).

64. Ward, V. C. A., Chatzivasileiou, A. O. & Stephanopoulos, G. Cell free biosynthesis of isoprenoids from isopentenol. *Biotechnol. Bioeng.* **116**, 3269–3281 (2019).

65. Chatzivasileiou, A. O., Ward, V., Edgar, S. M. & Stephanopoulos, G. Two-step pathway for isoprenoid synthesis. *Proc. Natl. Acad. Sci.* **116**, 506–511 (2019).

66. Lund, S., Hall, R. & Williams, G. J. An Artificial Pathway for Isoprenoid Biosynthesis Decoupled from Native Hemiterpene Metabolism. *ACS Synth. Biol.* **8**, 232–238 (2019).

67. Zheng, Y. *et al.* Metabolic engineering of Escherichia coli for high-specificity production of isoprenol and prenol as next generation of biofuels. *Biotechnol. Biofuels* **6**, 57 (2013).

68. George, K. W. *et al.* Metabolic engineering for the high-yield production of isoprenoid-based C5 alcohols in E. coli. *Sci. Rep.* **5**, 11128 (2015).

69. Kang, A. *et al.* Optimization of the IPP-bypass mevalonate pathway and fed-batch fermentation for the production of isoprenol in Escherichia coli. *Metab. Eng.* **56**, 85–96 (2019).

70. Kang, A. *et al.* Isopentenyl diphosphate (IPP)-bypass mevalonate pathways for isopentenol production. *Metab. Eng.* **34**, 25–35 (2016).

71. Thomas, S. T., Louie, G. V., Lubin, J. W., Lundblad, V. & Noel, J. P. Substrate Specificity and Engineering of Mevalonate 5-Phosphate Decarboxylase. *ACS Chem. Biol.* **14**, 1767–1779 (2019).

72. Laohakunakorn, N. Cell-Free Systems: A Proving Ground for Rational Biodesign. *Front. Bioeng. Biotechnol.* **8**, (2020).

73. Chen, K. & Arnold, F. H. Engineering new catalytic activities in enzymes. *Nat. Catal.* **3**, 203–213 (2020).

74. Wang, X. *et al.* Creating enzymes and self-sufficient cells for biosynthesis of the non-natural cofactor nicotinamide cytosine dinucleotide. *Nat. Commun.* **12**, 2116 (2021).

75. King, E., Maxel, S. & Li, H. Engineering natural and noncanonical nicotinamide cofactor-dependent enzymes: design principles and technology development. *Curr. Opin. Biotechnol.* **66**, 217–226 (2020).

76. Invizyne Technologies | arpa-e.energy.gov. https://arpa-e.energy.gov/technologies/projects/carbon-negative-chemical-synthetic-biochemistry.

77. Heyes, D. J. *et al.* Photochemical Mechanism of Light-Driven Fatty Acid Photodecarboxylase. *ACS Catal.* **10**, 6691–6696 (2020).

78. Khan, M. I., Shin, J. H. & Kim, J. D. The promising future of microalgae: current status, challenges, and optimization of a sustainable and renewable industry for biofuels, feed, and other products. *Microb. Cell Factories* **17**, 36 (2018).

79. Hannon, M., Gimpel, J., Tran, M., Rasala, B. & Mayfield, S. Biofuels from algae: challenges and potential. *Biofuels* **1**, 763–784 (2010).

80. Arbing, M. A. *et al.* Heterologous Expression of Mycobacterial Esx Complexes in Escherichia coli for Structural Studies Is Facilitated by the Use of Maltose Binding Protein Fusions. *PLOS ONE* **8**, e81753 (2013).

81. Goldenzweig, A. *et al.* Automated Structure- and Sequence-Based Design of Proteins for High Bacterial Expression and Stability. *Mol. Cell* **63**, 337–346 (2016).